Glycobiology Advance Access published September 1, 2016

THE CONUNDRUM OF UDP-Glc ENTRANCE INTO THE YEAST ER LUMEN

Luis M. Bredeston[ǁ]**,** Department of Biological Chemistry and IQUIFIB (CONICET), School of Pharmacy and Biochemistry, University of Buenos Aires, Buenos Aires C1113AAD, Argentine; **Cristina Marino-Buslje**[ǁ]**,** Fundación Instituto Leloir and IIBBA, CONICET, Buenos Aires C1405BWE, Argentine; **Vanesa S. Mattera,** Fundación Instituto Leloir, Buenos Aires C1405BWE, Argentine; **Lucila I. Buzzi,** Fundación Instituto Leloir, Buenos Aires C1405BWE, Argentine; **Armando J. Parodi*** Fundación Instituto Leloir and IIBBA, CONICET, Buenos Aires C1405BWE, Argentine; and **Cecilia D'Alessio*,** School of Sciences, University of Buenos Aires and Fundación Instituto Leloir and IIBBA, CONICET, Buenos Aires C1405BWE, Argentine.

[ǁ] Equal contribution

***To whom correspondence should be addressed**: Armando J. Parodi and Cecilia D'Alessio, Fundación Instituto Leloir, Av. Patricias Argentinas 435, Buenos Aires, Argentine C1405BWE. Telephone: (+5411) 5238-7500 ext 2302; fax: (+5411) 5238-7501; E-mail: cdalessio@leloir.org.ar or aparodi@leloir.org.ar.

Author for proofs and reprints: Cecilia D'Alessio

Running title: UDP-Glc entrance into the yeast ER

Keywords: Endoplasmic reticulum (ER) / *N*-linked glycosylation / nucleotide-sugar transporter / *Schizosaccharomyces pombe* / UDP-Glc

Supplementary data included: Table S1. Experimentally characterized NST.

ABSTRACT

UDP-Glc entrance into the endoplasmic reticulum (ER) of eukaryotic cells is a key step in the quality control of glycoprotein folding, a mechanism requiring transfer of a Glc residue from the nucleotide sugar to glycoprotein folding intermediates by the UDP-Glc:glycoprotein glucosyltransferase (UGGT). According to a bioinformatics search there are only eight genes in the *Schizosaccharomyces pombe* genome belonging to the three Pfam families to which all known nucleotide sugar transporters (NST) of the secretory pathway belong. The protein products of two of them (*hut1*$^+$ and *yea4*$^+$) localize to the ER, those of genes *gms1*$^+$, *vrg4*$^+$, *pet1*$^+$, *pet2*$^+$ and *pet3*$^+$ to the Golgi, whereas that of *gms2*$^+$ has an unknown location. Here we demonstrate that: 1) *Δhut1* and *Δgpt1* (UGGT null) mutants share several phenotypic features; 2) *Δhut1* mutants show a 50% reduction in UDP-Glc transport into ER-derived membranes; 3) *in vivo* UDP-Glc ER entrance occurred in *Δhut1Δyea4Δgms2* mutants and in cells in which *Δhut1* disruption was combined with that of each of four of the genes encoding Golgi-located proteins. We conclude that the *hut1*$^+$ gene product is involved in UDP-Glc entrance into the ER, but that at least another as yet unknown NST displaying an unconventional sequence operates in the yeast secretory pathway as disruption of all genes whose products localize to the ER or have an unknown location did not obliterate UDP-Glc ER entrance. This conclusion agrees with our previous results showing that UDP-Glc entrance into the yeast ER does not follow the classical NST antiport mechanism.

INTRODUCTION

Entrance of nucleotide sugars (NS[†]) into the secretory pathway of eukaryotic cells is essential for the correct biosynthesis of glycosidic compounds including glycoproteins. It is mediated by nucleotide sugar transporters (NST) that are 300-400 amino acid polytopic proteins embedded in the endoplasmic reticulum (ER) or Golgi membranes. Entrance of a NS (GDP-Man, UDP-Glc, UDP-Gal, UDP-GlcNAc, etc.) is coupled to the equimolar exit of the corresponding nucleoside monophosphate (GMP, UMP, etc.) (Hirschberg *et al.*, 1998). This antiport mechanism implies the conversion of the nucleoside diphosphate produced by the monosaccharide transfer reaction catalyzed by glycosyltransferases to the corresponding nucleoside monophosphate by luminal nucleoside diphosphatases (Berninsone *et al.*, 1994). The occurrence of nucleoside diphosphatases is not required in the case of CMP-sialic acid transport as in this case the monophosphate is directly produced upon sialic acid transfer (Milla & Hirschberg, 1989). Mutations in NST- or nucleoside diphosphatase-encoding genes results in decreased NS entrance into the secretory pathway and thence in modifications in the structure of protein- and lipid-linked oligo- and polysaccharides, that may produce in turn distinct phenotypes and even lethality (Liu *et al.*, 2010). Although it was assumed initially that individual NSTs were specific for a single NS, further work showed that in several cases the same NST was able to transfer different NSs, even with either purine or pyrimidine bases (Liu *et al.*, 2013). In addition, certain NSTs appeared to transport two different NS simultaneously, that is, one of them not inhibiting transport of the other (Caffaro *et al.*, 2006). There are NSTs of known specificity but unknown physiological role. For instance the occurrence of a NST specific for UDP-GlcNAc has been reported to occur in both *Saccharomyces cerevisiae* and *Schizosaccharomyces pombe* ERs (Roy *et al.*, 2000), but no GlcNAc transfer reaction is known to occur in that subcellular location. Synthesis of chitin in the budding yeast is known to occur on the cytosolic side of the plasma membrane whereas *S. pombe* totally lacks that polysaccharide (Horisberger *et al.*, 1978, Martin-

Garcia *et al.*, 2003). Those NSTs may be considered to be transfer-reaction orphans. Alternatively, the possibility exists that those NSTs transport, in addition to the already known one, a yet untested NS whose transfer reaction is already known.

Most of the already characterized NSTs localize to the Golgi, where they are required for the extensive processing of protein- and lipid-linked glycans. NSTs have nevertheless also been reported to occur in the ER, as for instance that responsible for entrance of UDP-Glc in plants (Blanco-Herrera *et al.*, 2015). In this subcellular location UDP-Glc is required for the quality control of glycoprotein folding, in which monoglucosylated *N*-glycans are recreated by the UDP-Glc:glycoprotein glucosyltransferase (UGGT), a glycoprotein folding sensor which tags glycans in folding intermediates with a Glc residue (D'Alessio *et al.*, 2010). The epitope created by the enzyme may be recognized by two ER-resident lectins, calnexin and calreticulin. The interaction of the lectins with monoglucosylated glycoproteins prevents exit of folding intermediates and irreparably misfolded glycoproteins to the Golgi and enhances the folding efficiency of the former. On glucosidase II-mediated deglucosylation the glycoprotein would be free to continue its travel through the secretory pathway or if still not properly folded would be re-glucosylated by the UGGT (D'Alessio *et al.*, 2010).

It is worth mentioning that according to what is known from *S. pombe* glycoconjugates, three different NSs have to enter into the secretory pathway: UDP-Glc into the ER for providing the substrate to UGGT and GDP-Man and UDP-Gal for the Golgi synthesis of both an *N*-linked galactomannan and O-linked short galactomanno glycans (Tanaka & Takegawa, 2001). Although it is possible that, as stated above, in certain known cases the same NST may transport different NSs containing either purine or pyrimidine bases and thence both GDP-Man and UDP-Gal might be transported by the same Golgi NST, evidence provided by Ohashi and Takegawa (Ohashi & Takegawa, 2010) and by results reported here show that each NS is transported by unique Golgi transporters. In the case of *S. cerevisiae* only one of them, a GDP-

Man transporter, would be apparently required for the Golgi synthesis of *N*-linked mannan, *O*-linked short glycans and mannolipids. Remarkably, although *S. cerevisiae* lacks UGGT, we have previously detected entrance of UDP-Glc into its ER (Castro *et al.*, 1999). The ER UDP-Glc transporter which provides substrate for UGGT has not yet been characterized in yeast.

In this paper we show entrance of UDP-Glc into the yeast ER to be the first case not involving either conventional NSTs or antiport mechanisms.

RESULTS

The Pfam protein families of NSTs with experimentally known specificities

It is not possible to determine the NS transported by a NST by pairwise sequence comparison as in some cases NSTs of related species that transport different NS may show a higher identity than NSTs from distant species that transport the same NS. We therefore tackled the identification of the NST involved in UDP-Glc entrance into the *S. pombe* ER lumen using a different bioinformatics approach.

The Pfam database is a large collection of protein domain families. Each family is represented by multiple alignments and hidden Markov models (HMM) (Finn *et al.*, 2014). Each Pfam family consists of a curated seed alignment containing a small set of representative members of the family, profile HMMs built from the seed alignment and a full alignment, which contains all detectable protein sequences belonging to the family, as defined by profile HMM searches of primary sequence databases (Finn *et al.*, 2016).

Nomenclature in the literature uses several databases, a fact that results in sequence comparison being a very cumbersome task. Therefore, we made a list of all NSTs from mammalian, fungal, plant, worm, insect and protozoan cells whose NS specificities have been

experimentally characterized including one of *S. pombe* (60 up to now) and mapped the several database IDs to unique UniProt IDs (UniProt Consortium, 2015) (Table S1).

Sequence analysis showed that NSTs of known specificity belong to only four Pfam families: PF08449 (UAA, transporter family), PF04142 (NST, nucleotide sugar transporters), PF03151 (TPT, triose phosphate transporters) and PF00153 (mitochondrial carrier proteins). It should be mentioned that the two protein sequences belonging to Pfam family PF00153 in Table S1 correspond to ADP-Glc transporters present in plastids, not in the secretory pathway (Kirchberger *et al.*, 2007, Soliman *et al.*, 2014). We then ran a BLAST search with each of the proteins of Table S1 (except for those two mentioned above) as queries against UniprotDB restricting the search to *S. pombe* genome. As a result, we recruited seven BLAST hits retrieved with at least one query which belong to the first three Pfam families mentioned above (Table III). By inspecting each of the three Pfam families we identified an additional *S. pombe* protein belonging to one of them (*gms2*$^{+}$, UniProt accession YAGC_SCHPO, Pfam family PF04142) that although not retrieved in the BLAST search was also included in our analysis.

Probable roles and subcellular localizations of eight S. pombe proteins belonging to the Pfam families PF08449, PF04142 and PF03151

Table III shows the Pfam families, UniProt accession, gene names, reference sequence accession numbers, and systematic identifications of the eight *S. pombe* genes belonging to the three Pfam families mentioned above as well as the subcellular localizations of their products established either by the *S. pombe* Orfeome Localization Database (PLD) (Matsuyama *et al.*, 2006) or by additional approaches. The product of gene *hut1*$^{+}$ (HUT1_SCHPO) has been localized to the ER by the PLD. Moreover, the protein displays the C-terminal consensus sequence for ER-localized membrane proteins (KKAS). The *S. cerevisiae hut1*$^{+}$ homologous gene has been tentatively identified as that encoding the UDP-Gal NST, although its deletion did not affect glycoprotein galactosylation and it localizes to the ER (see below) (Kainuma *et al.*,

2001, Nakanishi *et al.*, 2001). Gene *yea4*$^{+}$ (YEA4_SCHPO) has been functionally characterized in *S. cerevisiae* but not in *S. pombe*. In the budding yeast, it codes for an UDP-GlcNAc (but not UDP-Gal or GDP-Man) transporter and localizes to the ER by immunofluorescence (Roy *et al.*, 2000). The same localization has been determined for the product of its *S. pombe* homologue by the PLD (Matsuyama *et al.*, 2006). Moreover, both the *S. cerevisiae* and *S. pombe yea4*$^{+}$ genes display the KKxx sequence at their C-termini. The gene *vrg4*$^{+}$ (GMT_SCHPO) codes for the GDP-Man transporter which localizes to the Golgi (see below) (Dean *et al.*, 1997). Of the eight *S. pombe* genes belonging to the three Pfam families, *gms1*$^{+}$ (GMS1_SCHPO) is the only one whose product has been characterized as a NST (Segawa *et al.*, 1999). It belongs to the Pfam family PF04142 and transports UDP-Gal. Furthermore, its null mutants are deficient in the incorporation of Gal to galactomannoproteins, a Golgi process (Ohashi & Takegawa, 2010), and the protein localizes to the Golgi as determined by indirect immunofluorescence (Tanaka & Takegawa, 2001). Concerning the product of the remaining *S. pombe* gene belonging to Pfam family PF04142 (*gms2*$^{+}$, YAGC_SCHPO) nothing is known, not even its subcellular localization. The products of two of the *S. pombe* genes belonging to Pfam family PF03151 (*pet1*$^{+}$ and *pet2*$^{+}$: YIY4_SCHPO and YG1B_SCHPO, respectively) have been identified as phophonenolpyruvate (PEP) transporters (Yoritsune *et al.*, 2014). PEP is responsible for pyruvylation of the galactomannan in the Golgi. As expected, both expression of their GFP-linked derivatives and the PLD showed that they localize to the Golgi. On the other hand, although the role of the product of gene *pet3*$^{+}$ (YDB1_SCHPO) is unknown, it has been localized to the Golgi by the PLD (Matsuyama *et al.*, 2006). In conclusion, from the eight putative NSTs codified in *S. pombe* genome, only those encoded by *hut1*$^{+}$ and *yea4*$^{+}$ have been localized to the ER and only *gms1*$^{+}$ and *vrg4*$^{+}$ products (see below) have been identified as UDP-Gal and GDP-Man transporters, respectively.

Vrg4^{+} *codes for a GDP-Man transporter localized to the Golgi*

We identified *vrg4*$^{+}$ as the GDP-Man transporter-encoding gene because: a) it displays the sequence W*XXX*TTYS*X*VG(A/S)LNK(L/IP) that has been identified as that binding the NS in GDP-Man transporters present in other organisms (Gao *et al.*, 2001) and b) labeling of wild type or *Δvrg4* mutants with [^{14}C]Glc followed by isolation of the cell wall and further strong acid hydrolysis and paper chromatography revealed the presence of Gal, Glc and Man in the case of wild type cells and of only Glc in that of the *Δvrg4* mutant (Fig. 1*A,B*). This result is consistent with a defect in the formation of cell wall galactomannan, which is synthesized in the secretory pathway and requires entrance of GDP-Man into the Golgi lumen. Furthermore, the products of *S. cerevisiae* and *Candida glabrata vrg4*$^{+}$ homologous genes that display the above mentioned GDP-Man-binding sequence have been reported to localize to the Golgi (Dean *et al.*, 1997, Nishikawa *et al.*, 2002). In *S.pombe* galactomannan one or two Gal units are added as non-reducing ends to a polymannose polymer (Ohashi & Takegawa, 2010). A variety of different glucans, which are additional cell wall components, are mainly if not entirely, formed on the cytosolic face of the plasma membrane. Furthermore, as expected for mutants affected in cell wall synthesis, *Δvrg4* mutants display growth deficiencies, morphological aberrations and agglutination tendency (Fig. 1*C,D*).

As mentioned above, the known structures of protein-linked oligo- and polysaccharides occurring in *S. pombe* only require the expression of three NSTs, those responsible for UDP-Glc, UDP-Gal and GDP-Man transport. Results presented above as well as those reported in (Tanaka & Takegawa, 2001) indicate that the last two have already been identified and localize to the Golgi.

Construction of NST similarity networks

To infer protein family and sequences interrelationships, similarity networks are better tools than phylogenetic trees as they retain the basic clustering and topology information present in the

latter and at the same time show the multiple neighbors of given sequences. Moreover, the networks can reveal sequences that may have sequence characteristics useful for linking divergent clusters in multiple alignments (Atkinson *et al.*, 2009).

Sequence similarity networks were constructed for the 67 sequences comprising experimentally characterized NSTs (Table S1) and *S. pombe* putative transporters shown in Table III. In a thresholded sequence similarity network, sequences are represented as nodes (circles) and all pairwise sequence relationships (alignments) better than a given threshold as edges (lines). Figures 2*A*-*E* show the similarity network at different thresholds. As thresholds get more stringent, the sequences break up into disconnected groups and within each group the sequences show higher similarity.

In the first panel (Fig. 2A) the network has no threshold (all the pairwise BLAST E-values are displayed). This means that every two sequences are compared by BLAST and this comparison has an E-value, even if they are unrelated. Therefore, in the unthresholded network the score does not reflect similarity and the network should only be taken as a starting point. The more related the sequences are, the smaller is the E-value. In such a way in an initial step (Fig. 2A) all proteins are connected, while when setting a threshold (Figs. 2 B-E), the more distantly related proteins at a given threshold are disconnected from the network. Sequences belonging to the same Pfam family are of the same color. Green was exclusively used for all *S. pombe* sequences irrespective of the Pfam family to which they belong. In Fig. 2*B* the network was thresholded at a BLAST E-value of $1x10^{-10}$ that corresponds to a sequence identity value of about 25% for an alignment length of about 300-400 amino acids. Thus, only edges associated with E-values more significant than $1x10^{-10}$ are included in the network.

Similarly, in Fig. 2*C* the network was thresholded at a BLAST E-value of $1x10^{-20}$. The worst edges displayed correspond to 28 % sequence identity. Figs. 2*D* and 2*E* show E-values thresholds of $1x10^{-25}$ (about 32% identity) and $1x10^{-35}$ (about 33% identity), respectively. Several

intermediate thresholds have been analyzed (data not shown), though the more meaningful ones are those shown.

It may be observed that sequences belonging to Pfam family PF00153 (colored pink in Fig. 2) disaggregate from the similarity network at early stringency values. This is to be expected as they code for ADP-Glc transporters of plastids, not of secretory pathway organelles as all the others. It may also be observed that Pfam family PF04142, (colored red in Fig. 2) is a cohesive and homogeneous group of sequences that remain clustered even under very stringent conditions. On the contrary, sequences belonging to Pfam families PF08449 (colored violet in Fig. 2) and PF03151, (colored yellow in Fig. 2) do not settle in a unique cluster and some sequences are more similar to sequences of the other families than to other members of the same Pfam family. More sub-groups are formed when thresholds that are more stringent are applied. It is worth mentioning that we also ran a PSI-BLAST search for identifying *S. pombe* genes encoding NSTs, with an E-value set at $1x10^{-3}$ and three iterations. Only one new *S. pombe* protein appeared at the third iteration. The sequence corresponds to sequence NP_587721 (UniProt accession ID YCN8_SCHPO). The 505 amino acid protein belongs to a Pfam family (PF06027) different from the three families to which all known NSTs belong and it matches only in part of the sequence (residues 100 to 220 approximately) with a marginal score. According to the Orfeome Localization Database the protein localizes to the Golgi periphery, especially at the cell tip and site of septum formation and in the vacuolar membrane. Inclusion of YCN8_SCHPO sequence in an analysis similar to that depicted in Fig. 2 showed that this sequence was disconnected from the network at a threshold E-value of $1x10^{-2}$. This value is similar to those of proteins belonging to Pfam family PF00153 present in plant plastids, not in the secretory pathway ($1x10^{-1}$). *S. pombe* proteins belonging to the three Pfam families to which all NSTs belong but whose roles are either unknown (products of genes *gms2*$^+$ and *pet3*$^+$) or they correspond to phosphoenolpyruvate transporters (products of genes *pet1*$^+$ and *pet2*$^+$)

were disconnected at values of $1x10^{-9}$ and $1x\ 10^{-25}$, respectively. Sequences of known *S. pombe* secretory pathway NSTs (products of genes *hut1*$^+$, *vrg4*$^+$, *yea4*$^+$ and *gms1*$^+$) were not disconnected even at E-values of $1x10^{-40}$. As protein YCN8_SCHPO was disconnected from the network at a very early threshold E-value and it localizes to the Golgi, we did not add it to either the sequence (Fig. 2) or genetic analysis (Figs, 3, 4, 6 and 7).

Four S. pombe genes may be assigned to well-defined NST clusters

We then superimposed the substrate specificity of each NST (Table S1) with that of the clustering in the similarity network: in Fig. 2*E* each gene product has a small colored star attached indicating the NS transported. It may be observed that under the more stringent condition *gms1*$^+$ (the *S. pombe* gene coding for an UDP-Gal transporter) is included in a group whose members predominantly transport UDP-Gal, *vrg4*$^+$ (the *S. pombe* gene coding for a GDP-Man transporter) in a group whose members exclusively transport GDP-Man, *yea4*$^+$ in a group whose products only transport UDP-GlcNAc and finally, *hut1*$^+$ is included in a group whose product transport UDP-Glc and/or UDP-Gal. It is interesting to notice that members of the same Pfam family may transport different NSs, and members of different Pfam families may transport the same NS. This result shows why it is so problematic to predict the substrate specificity of NST from the amino acid sequence. However, the similarity network clearly shows that members of the same or different families that transport the same NS tend to cluster. In this analysis Pfam PF04142 is the most homogenous family regarding both family member clustering and NS transported by its members. Products of genes *gms2*$^+$, *pet1*$^+$, *pet2*$^+$ and *pet3*$^+$ disaggregated from the similarity network before reaching the more stringent conditions. As mentioned above, products of genes *pet1*$^+$, *pet2*$^+$ and *pet3*$^+$ localize to the Golgi, thus suggesting that it is unlikely that they are involved in UDP-Glc transport into the ER. Both the bioinformatics analysis of genes and subcellular localization of their products point, therefore, to *hut1*$^+$ as the gene encoding the UDP-Glc ER transporter. Nevertheless, at this point it cannot be

absolutely ruled out that the product of gene *gms2*$^{+}$, a protein of unknown role and subcellular localization, or even of other genes mentioned in Table III could also display UDP-Glc transport activity.

S. pombe Δalg5Δhut1 and Δalg5Δgpt1 mutants share phenotypic defects

We have previously reported that UGGT (coded by *gpt1*$^{+}$ gene) is required for survival of *S. pombe* under conditions of severe ER stress, as combining protein underglycosylation and high temperature (Fanchiotti *et al.*, 1998). The *alg5*$^{+}$ and *alg6*$^{+}$ genes code for the enzymes that synthesize dolichol-P-Glc or that transfer the first Glc from this last compound to $Man_9GlcNAc_2$-P-P-dolichol, respectively. Therefore, null mutants of either one of both genes transfer $Man_9GlcNAc_2$ to proteins instead of $Glc_3Man_9GlcNAc_2$, thus resulting in glycoprotein underglycosylation and, therefore, in protein folding defects and induction of the unfolded protein response. *Δalg5Δgpt1* or *Δalg6Δgpt1* double mutants cannot enter into the calnexin/calreticulin cycle as they never produce monoglucosylated species required for interaction with those lectins. They are viable unless an additional stress as high temperature is introduced. Both double mutants mentioned above grow slowly and show a rounded aberrant morphology at 28 ^{o}C and are unable to grow at 35 ^{0}C (Fanchiotti *et al.*, 1998).

We hypothesized that cells showing glycoprotein underglycosylation would display the same phenotype whether they also lacked UGGT or were deficient in UDP-Glc entrance into the ER lumen. We thus generated *S. pombe* double mutants of genes whose sequences belonged to the three Pfam families shown in Table III combined with *Δalg5.* Only *Δalg5Δhut1* showed the same growth phenotype as *Δalg5Δgpt1* (Fig. 3). No double mutants involving *Δvrg4* (GDP-Man transporter gene) were constructed as even the single mutant grows very poorly at 35 ^{0}C (Fig. 1*C*).

Similarly, *Δalg5Δhut1* was the only double mutant that showed an aberrant clumping morphology similar to that of *Δalg5Δgpt1* when grown at 28 ^{0}C (Fig. 4). On the other hand, the *Δvrg4* mutant displayed an aberrant morphology at 28 ^{0}C even when not combined with *Δalg5* (Fig. 1*D*).

UDP-Glc entrance into S. pombe ER-derived vesicles

Entrance of glucose-labeled UDP-Glc into *S. pombe* ER vesicles prepared by cell disruption followed by ultra- and sucrose gradient- centrifugations was assayed by two different methods. In the first, vesicles were incubated with the labeled NS at 0 ^{0}C or 30 ^{0}C, the reactions were then stopped with cold buffer and the vesicles were ultracentrifuged. The pellets were then resuspended and ultracentrifuged four more times. The vesicles were the lysed and label in the supernatants was quantified. The second method is simpler: after incubations at 0 ^{0}C or 30 ^{0}C, ER vesicles were diluted with cold buffer, the suspension filtered through a cellulose acetate filter and extensively washed with the same buffer. Label in the filter was then quantified. In both methods values obtained at 0 ^{0}C were subtracted from those obtained at 30 ^{0}C. Strains used were *Δalg5* and *Δalg5ΔhutΔyea4* or *Δalg6* and *Δalg6Δhut1*. As depicted in Fig. 5*A,B*, approximately a 50 % reduction in UDP-Glc entrance into vesicles was observed in both cases in strains having the *Δhut1* deletion. It should be noted that the products of *hut1*$^+$ and *yea4*$^+$ genes are apparently the only ones that localize to the ER and that the bioinformatics analysis and the phenotype of the *Δalg5Δhut1* double mutant (see above) strongly suggest that *hut1*$^+$ might be the gene coding for the UDP-Glc transporter. Moreover, the fact that *Δalg5Δhut1Δyea4 and Δalg6Δhut1* strains gave the same result is not surprising because as mentioned above the *yea4*$^+$ gene tentatively encodes for an UDP-GlcNAc transporter and both *Δalg5* and *Δalg6* mutations result in similar protein underglycosylations.

Results shown in Fig. 5*A,B* suggest that there is at least one additional transporter for UDP-Glc besides that encoded by *hut1*$^+$. It cannot be ruled out, however, that *hut1*$^+$ is not a UDP-Glc

transporter encoding gene but that its ablation reduces the expression or activity of the true transporter.

At least part of UDP-Glc entrance into the yeast ER is not mediated by a transporter belonging to the same Pfam families of other known NSTs of the secretory pathway

Results obtained so far strongly suggest that there is an additional transporter responsible for UDP-Glc entrance into the *S. pombe* ER lumen, besides that encoded by *hut1*$^{+}$. To confirm this suggestion we determined the *N*-linked glycan pattern of glycoproteins in either *S. cerevisiae* or *S. pombe* mutants deficient in dolichol-P-Glc formation (*Δalg5*) harboring in addition mutations in genes belonging to the three Pfam families shown in Table III. We incubated the cells for 15 min with 5 mM [^{14}C]Glc in the presence of 5 mM DTT and 5 mM NMDNJ, 8 mM CST. Under conditions employed incorporation of label into *N*-linked glycans is dependent on incubation time, passage of newly synthesized glycoproteins from the ER to the Golgi (and thus incorporation of Gal units into glycoproteins) is prevented by DTT that interferes in disulfide bond formation and thus in glycoprotein folding (Braakman *et al.*, 1992), and glucosidase II activity is totally inhibited by NMDNJ and CST. In the case of the budding yeast we also expressed *S. pombe* UGGT as *S. cerevisiae* lacks this enzyme. The protocol used ensures that formation of protein-linked $Glc_1Man_9GlcNAc_2$ is exclusively mediated by UGGT activity and is, therefore, an indication of UDP-Glc occurrence in the ER lumen as both UGGT and its substrates (folding intermediates) localize to that subcellular location. As shown in Fig. 6*A,B*, both $Man_9GlcNAc_2$ and $Glc_1Man_9GlcNAc_2$ were labeled in *S. pombe Δalg5* mutant but only the non-glucosylated compound appeared when the double mutant *Δalg5Δgpt1* was used. This result confirms that formation of the monoglucosylated compound was dependent on UGGT activity. It is worth mentioning that the assay is able to detect the presence of UDP-Glc in the ER lumen but not its concentration or entrance rate. Label in monoglucosylated glycans not only depends on the NS concentration but also on that of the acceptor substrates (folding

intermediates). The possible effect of the different mutations introduced on folding efficiency (i.e: folding intermediate concentration) is presently unknown. In addition, the specific activities of [^{14}C]Glc and [^{14}C]Man may differ in the different mutants. We then tested formation of $Glc_1Man_9GlcNAc_2$ in both *S. pombe* and *S. cerevisiae* strains harboring the *Δalg5* deletion plus that of the other genes whose products are known to localize to the ER (*Δhut1* and *Δyea4*). As shown in Fig. 6*C-F* the double mutants *Δalg5Δhut1* and *Δalg5Δyea4* from both yeasts formed monoglucosylated *N*-glycans. It should be mentioned that *S. cerevisiae* expresses a highly active ER α-mannosidase that converts $Man_9GlcNAc_2$ to $Man_8GlcNAc_2$ as soon as the glycan is transferred to protein, whereas the corresponding *S. pombe* enzyme shows a much weaker activity (Jelinek-Kelly *et al.*, 1985, Movsichoff *et al.*, 2005). This explains why $Glc_1Man_9GlcNAc$ and $Glc_1Man_8GlcNAc$ appear in *S. pombe* and *S. cerevisiae* protein-linked *N*-glycan patterns, respectively (Figs. 6 C,E and 6 D,F).

As the possibility exists that entrance of UDP-Glc into the ER lumen could be mediated by an additional transporter besides that encoded by *hut1*$^+$, we assayed formation of monoglucosylated glycans in the *S. pombe* triple and quadruple mutants *Δalg5Δhut1Δyea4* and *Δalg5Δhut1Δyea4Δgms2*. In the former strain all genes coding for NSTs known to localize to the ER membrane had been deleted and in the latter the only gene encoding a protein of unknown localization had been additionally disrupted (all other gene products depicted in Table III localize to the Golgi). As shown in Fig 7A,B monoglucosylated glycans were formed in both triple and quadruple mutant strains. It may be concluded that UDP-Glc enters the ER lumen through an unconventional transporter. To confirm this conclusion we assayed monoglucosylated glycan formation in triple mutants bearing *Δalg5* and *Δhut1* disruptions plus those of each of other genes depicted in Table III even though their products are known to localize to the Golgi (*Δgms1*, *Δpet1*, *Δpet2* and *Δpet3*). Monoglucosylated glycans were formed in all cases (Fig. 7C-F). *Vrg4*$^+$ was the only *S. pombe* gene of the eight ones belonging to the three Pfam families

with which a deletion mutant combined with the *Δalg5* mutation could not be constructed, probably because of the growth deficiencies observed in the respective single mutants even at 28 ^{0}C. Nevertheless, the product of *vrg4*$^{+}$ gene is unlikely to be involved in UDP-Glc transport because, as reported above, it encodes a GDP-Man transporter and localizes to the Golgi and not to the ER. The possibility that *vrg4*$^{+}$ encodes a NST transporting both GDP-Man and UDP-Glc, and that the last NS could be sent from the Golgi to the ER by retrograde vesicular transport also seems unlikely, as we have previously reported that monoglucosylated glycans were formed in the ER of *S. cerevisiae Δalg5* mutants in which retrograde transport had been blocked by a thermosensitive mutation (D'Alessio *et al.*, 2005). In all cases, strong acid hydrolysis of the *N*-glycans followed by paper chromatography showed that Glc and Man but not Gal were the monosaccharide constituents, thus showing that DTT had effectively prevented passage of glycoproteins to the Golgi (Fig. 8A-J).

DISCUSSION

The bioinformatics search and the NST similarity network we constructed indicated that *hut1*$^{+}$ was most probably a *S. pombe* gene encoding an UDP-Glc transporter. The double mutant *Δalg5Δgpt1* that synthesized underglycosylated glycoproteins due to an inefficient transfer of glycans to proteins and that lacked UGGT displayed phenotypic features similar to those of *Δalg5Δhut1*, thus suggesting that the absence of the *hut1*$^{+}$ protein product resulted in an impaired UGGT activity. Direct measurement of UDP-Glc entrance into ER-derived vesicles by two different methods showed that disruption of *hut1*$^{+}$ resulted in a 50 % decrease in the NS transport, thus indicating that the gene product might be an UDP-Glc transporter. However, as mentioned above, it cannot be ruled out that the *hut1*$^{+}$ protein product might not be an UDP-Glc transporter but that deletion of the gene results in a decreased expression or activity of the true transporter. The *S. cerevisiae hut1*$^{+}$ homologue has been tentatively identified as a gene encoding an UDP-Gal transporter as its overexpression resulted in a three-fold increase in

UDP-Gal entrance into ER-plus Golgi-derived vesicles (Kainuma *et al.*, 2001). Again, this effect might be an indirect consequence of expressing the protein in the ER (Nakanishi *et al.*, 2001). The fact that *hut1*$^+$ deletion did not abolish galactosylation of an ill characterized glycoconjugate (Kainuma *et al.*, 2001) supports this last speculation. In addition, it cannot be excluded that the *hut1*$^+$ protein product might be both an UDP-Glc and UDP-Gal transporter or that it could be an UDP-Gal transporter in *S. cerevisiae* and an UDP-Glc transporter in *S. pombe*. Nevertheless, the fact that *hut1*$^+$ disruption only results in a partial decrease in UDP-Glc entrance into ER-derived vesicles indicates that an additional transporter is operative in *S. pombe*. The aberrant growth features and morphologies shown by *Δalg5Δhut1* double mutants in Figs. 3 and 4 cannot be ascribed to protein underglycosylation plus a total UDP-Glc entrance deficiency as initially assumed because results displayed in Fig. 6 showed that the NS was indeed transported into the ER lumen in those mutants and that UGGT was operative. Whether results shown in Figs. 3 and 4 are a consequence of a reduced (but not null) UDP-Glc entrance into the ER lumen is an open question.

Entrance of UDP-Glc into the ER lumen was then assayed in intact cells. The assay was based on detection of monoglucosylated *N*-glycan formation ($Glc_1Man_9GlcNAc_2$ in *S. pombe* and $Glc_1Man_8GlcNAc_2$ *in S. cerevisiae*) in cells transferring $Man_9GlcNAc_2$ to proteins (*Δalg5* mutants). Formation of monoglucosylated *N*-glycans in those mutants is strictly dependent on UGGT activity, thence on the presence of both UDP-Glc and folding intermediate acceptor molecules in the same subcellular location (D'Alessio *et al.*, 2010). As both the enzyme and the intermediates localize to the ER lumen the assay provides a reliable indication on the occurrence of the NS in that subcellular location. The bioinformatics search showed that there are eight *S. pombe* genes belonging to the three Pfam families to which all 60 known and functionally characterized NSTs present in mammalian, plant, insect, protozoan and fungal cell secretory pathways belong. Two of the *S. pombe* gene protein products localize to the ER, five

to the Golgi and one has an unknown location. Formation of monoglucosylated *N*-glycans was detected not only in mutants in which all genes whose protein products localize to the ER had been disrupted (*Δalg5Δhut1Δyea4*), but also in a mutant in which the gene whose product has an unknown location had been additionally disrupted (*Δalg5Δhut1Δyea4Δgms2*). Furthermore, monoglucosylated *N*-glycans were also formed in mutants displaying a combination of *Δalg5Δhut1* disruption with those of each of four of the genes whose protein products localize to the Golgi. We also detected $Glc_1Man_8GlcNAc_2$ formation in *S. cerevisiae* mutants involving disruption of the respective homologues of *S. pombe Δalg5Δhut1* and *Δalg5Δyea4* double mutants in which we expressed *S. pombe* UGGT as the budding yeast lacks the enzyme (Fernandez *et al.*, 1994). It is worth mentioning that no known UDP-Glc transfer reaction is known to occur in *S. cerevisiae* ER as synthesis of dolichol-P-Glc, sterylglucoside, glycogen and cell wall glucans are known to occur in the cytosol. It may be concluded, therefore, that UDP-Glc enters at least partially into the yeast ER lumen through an unconventional NST not displaying a sequence similar to those of all known transporters.

We have previously provided evidence suggesting an unconventional mechanism for UDP-Glc entrance into the yeast ER (D'Alessio *et al.*, 2003, D'Alessio *et al.*, 2005). As mentioned above, the known antiport mechanism implies entrance of the NS and an equimolar exit of the nucleoside monophosphate. In the case where a nucleoside diphosphate is produced by the monosaccharide transfer reaction, a nucleoside diphosphatase converts the diphosphate to the monophosphate derivative. Ablation of nucleoside diphosphatase-encoding genes resulted in an impaired NST entrance into the secretory pathway lumen and thence in defective glycoprotein and lipid glycosylations (Abeijon *et al.*, 1993, Berninsone *et al.*, 1994). Nevertheless we found that no nucleoside diphosphatases localize to either *S. pombe* or *S. cerevisiae* ERs. Both yeasts express two Golgi proteins with diphosphatase activities, a diphosphatase proper and an apyrase (apyrases hydrolyze both di- and triphosphates). In the case of *S. pombe* only one of

both encoding genes could be deleted as deletion of both appeared to be lethal but in the case of *S. cerevisiae* deletion of both genes could be performed, thus resulting in cells totally devoid of nucleoside diphosphatase activities in the secretory pathway. Nevertheless either in *S. pombe* single or *S. cerevisiae* double mutants entrance of UDP-Glc into the ER was detected using a $Glc_1Man_9GlcNAc_2$ formation assay similar to that described in the present work (D'Alessio *et al.*, 2003, D'Alessio *et al.*, 2005). These results also strongly suggest UDP-Glc entrance into the yeast ER by an unconventional mechanism different from the already described antiport one. Furthermore, using *S. cerevisiae* thermosensitive mutants affected in both anterograde and retrograde vesicular traffic between the ER and Golgi we discarded the possibility that UDP produced in the ER by the UGGT-mediated reaction could be transported to the Golgi to be converted to UMP and this last nucleotide transported back to the ER lumen (D'Alessio *et al.*, 2005). How the yeast ER lumen relieves UGGT inhibition by UDP is presently unknown. On the other hand, a conventional antiport mechanism appears to be operative in the mammalian cell ER, a subcellular location known to harbor a resident nucleoside diphosphatase activity (Trombetta & Helenius, 1999). Moreover, plant and worm ER UDP-Glc transporters have been already characterized (Norambuena *et al.*, 2002, Caffaro *et al.*, 2008, Reyes *et al.*, 2010, Seino *et al.*, 2010). Their sequences show similarities higher to *hut1*$^+$ than to other *S. pombe* genes.

Entrance of UDP-Glc into the yeast ER appears to be, therefore, the first case not involving either conventional NSTs or antiport mechanisms.

MATERIALS AND METHODS

Sequence retrieval, search of homologues and sequence alignment

A list of transporters with probed NS transport activity was compiled by thoroughly searching the literature. Several database IDs were mapped to unique UniProt IDs for all the NSTs except for two that have no UniProt accession assigned and were identified as originally published as VvGONST-A and VvGONST-B, corresponding to XP_002271444.1 and XP_002284977.1 (Table S1). Their sequences were retrieved in FASTA format from UniProt (UniPark in the last two cases). This resulted in a set of 60 NSTs from different species (including *S. pombe* UDP-Gal transporter *gms1*$^{+}$) belonging to four Pfam families (Pfam 28.0 December 2015). A BLAST search with each of the proteins of Table S1 as queries (with the exception of the two genes belonging to family PF00153 that code for transporters present in plastids) against NCBI non-redundant database restricting the search to *S. pombe* genome was then performed. BLAST expected value threshold (E-value) was set as $1x10^{-3}$. This resulted in a set of seven BLAST hits in *S. pombe* (retrieved with different queries) belonging to three Pfam families. By searching in the UniProt database for all proteins included in each of the three Pfam families we identified an additional *S. pombe* protein belonging to one of them (UniProt accession YAGC_SCHPO, Pfam family PF04142, gene *gms2*$^{+}$) that although not retrieved in the BLAST search was also included in our analysis. Sequences were aligned with T-Coffee (Notredame *et al.*, 2000) and from this alignment an identity matrix was created with R (R Core Team, 2013). To confirm these results, three iterations of a PSI-BLAST search with an E-value set as $1x10^{-3}$ were run. An additional hit of *S. pombe* was retrieved belonging to Solute carrier protein family (PF06027). This protein was only retrieved at the third iteration, it is 505 residues long, and matches only part of the sequence (residues 100 to 220 approximately) with a marginal score, so it was not included in the analysis (see below).

Construction of a sequence similarity network

A sequence similarity network consists of a collection of edges corresponding to pairwise relationships that are better than a defined threshold (Atkinson *et al.*, 2009). We set the pairwise relationships as the E-value associated with a BLAST alignment (Altschul *et al.*, 1990, Atkinson *et al.*, 2009). A database (custom DB) with BLAST formatDB including in total 67 proteins was created: the sequences of 60 known NSTs (including *S. pombe gms1*$^{+}$) as well as the 7 new proteins retrieved from *S. pombe*. A BLAST all against all search in the database was then performed. Each BLAST pairwise alignment E-value was treated as an edge. However, by using a set of related proteins as a database, the background model assumption that similarity hits follows an extreme value distribution is violated. Thus, the BLAST E-value must be considered here as a type of score, rather than a true expectation value. That means that every two sequences are compared by BLAST and this comparison has an E-value, even if they are unrelated, so for some comparisons, this score does not reflect similarity and the network should only be taken as a starting point. The more related the sequences are, the smaller is the E-value. Sequence similarity networks in this work were visualized using Cytoscape, spring-embedded edge weighted layout (Shannon *et al.*, 2013). Thresholded sequence similarity networks represent sequences as nodes (circles) and all pairwise sequence relationships (alignments) better than a BLAST E-value threshold as edges (lines).

Materials

Bactotryptone, bactopeptone and yeast nitrogen base (YNB) were from Difco. Yeast extract, malt extract and agar were from Britania (Argentina). Glucose was from Biopack. Endo-β-*N*-acetylglucosaminidase H (Endo H), porcine trypsin, dithiothreitol (DTT), amino acids, protease inhibitors and supplements for culture media were from Sigma. Geneticin (G418) was from InvivoGen. Restriction enzymes were from New England Biolabs. Ligase was from Promega. Zymolyase 100T was from Sunrise Science products. [^{14}C]glucose (301 Ci/mol) was from

PerkinElmer Life Sciences. UDP-[^{3}H]Glc (60 Ci/mmol) was from American Radiolabeled Chemicals. UDP-[^{14}C]Glc (301 Ci/mol) was prepared as described by Wright and Robbins (1965). *N*-methyl-1-deoxynojirimycin (NMDNJ) and castanospermine (CST) were from Toronto Research Chemicals.

Strains and media

Escherichia coli DH5α cells, used for plasmid cloning purposes, were grown at 37 °C in LB medium (0.5 % NaCl, 1 % bactotryptone, 0.5 % yeast extract) supplemented with 200 µg/ml ampicillin or 50 µg/ml kanamycin as needed. *S. pombe* strains were grown at 28 °C in low adenine rich media YE (0.5 % yeast extract, 3 % glucose) when testing for *ade6* genotype, or in YES medium (YE medium supplemented with 75 mg/l adenine). Solid malt extract medium (3 % malt extract pH 5.5) was used for *S. pombe* matings. *S. pombe* were selected in EMM minimal medium (Moreno *et al.*, 1991, Alfa *et al.*, 1993) supplemented with adenine 75 mg/l, leucine 250 mg/l or uracil 75 mg/l as required. Geneticin was added to *S. pombe* media at 150 µg/ml for KanMX cassette selection in rich media. *S. cerevisiae* cells were grown and mated in YPDA medium (1% yeast extract, 2% bactopeptone, 2% glucose, supplemented with 20 mg/liter adenine) and selected in SD medium (0.67 % YNB without amino acids, 2% glucose) containing the required supplements (adenine, uracil, tryptophan, and histidine were added at 20 mg/liter; leucine and lysine were added at 30 mg/liter) or YPDA with 150 µg/ml geneticin. Solid media were made with 2% agar. The yeast strains used in this study are summarized in Tables I (*S. pombe*) and II (*S. cerevisiae)*.

DNA procedures

DNA procedures were as described previously (Sambrook & Russell, 2001). Yeast DNA extraction was performed as described previously (Hoffman & Winston, 1987). *S. pombe* transformations were performed by electroporation with 0.5 µg of plasmid DNA or 1 µg of linear

DNA as described (Stigliano *et al.*, 2009). *S. cerevisiae* transformations were performed by electroporation with 0.2 μg of plasmid DNA.

Construction of S. pombe mutants

S. pombe strains employed are summarized in Table I. Mutant ADpA was constructed the same as Sp61A (Stigliano *et al.*, 2009) but using the genetic background of ADp (Table I). *S. pombe* Sp61A6 *(Δalg6::Δura4)* mutant was constructed removing the *ura4*$^+$ cassette inserted in the partially deleted *alg6*$^+$ gene in Sp61A mutants *(Δalg6::ura4*$^+$*)* as follows: a fragment of 812 bp of *alg6*$^+$ gene (nucleotides 244 to 1056) cloned in pT7Blue vector was digested with BglII and BclI to remove 146 pb and then religated to generate a truncated version of the *alg6*$^+$ gene fragment, which in turn was liberated from the vector by digestion with KpnI and XbaI restriction enzymes. The fragment was transformed into Sp61A cells and selection of Ura$^-$ yeasts was performed in 5'fluororotic acid plates as described (Fernandez *et al.*, 1998). Homologous recombination between *alg6*$^+$ sequences flanking *ura4*$^+$ gene was verified by PCR using primers aca: 5'-CCAGAGCTAAAAGACGTTTAC-3' and acs: 5'-CGAATGGTTTGCTGATGT-3'.

S. pombe Δalg5 strain was constructed as follows: a disruption cassette containing the sequence of the *ura4*$^+$ *gene* flanked by 370 bp and 231 bp of the 5' and 3' portions of the *S. pombe alg5*$^+$ gene (SPBC56F2.10c) was obtained in two PCR rounds as described (Krawchuk & Wahls, 1999). In the first round two long primers containing sequences corresponding to the 5' and 3' coding regions of *alg5*$^+$ gene and 23-25 bases homologous to the *ura4*$^+$ *gene* were obtained with the primers W-alg5s1: 5'- GAGGAAGCAACTGGAAGGAG-3' / X-ura4-alg5a**:** 5'-GCCAGTGGGATTTGTAGCTAAGCTACAACATGCCCCAAGTTACC-3´ and Y-ura4-alg5s: 5'-CAAAAAGTTTCGTCAATATCACAAGCTTAGGGATCAGGGAGATTGG-3' / Z-alg5a: 5'-AGTAATACGCTTAGCCGAGG-3´ using genomic *S. pombe* DNA as template (regions homologous to *ura4*$^+$ are underlined). In the second round, both synthesized long primers were

used with an excess of primers W-alg5s1 and Z-alg5a to amplify the 2320 bp disruption cassette using the plasmid pBluescript-*ura4*$^+$ as the template. The resulting DNA was electroporated into competent *S. pombe* ADp cells, and homologous recombination in uracil prototroph colonies was confirmed by PCR with the primers alg5s1**:** 5´-CCTGCCTTGCGGGATTTATC-3' and uraAN: 5'-TTTTCATCCCCTCAGCTC-3' and by Southern blot using both a labeled probe synthesized by PCR using primers W-alg5s and Z-alg5a and a labeled probe of gene *ura4*$^+$ (to check for a single homologous recombination in the yeast genome). The resulting strain *Δalg5::ura4*$^+$ was called ADpA5 (Table I).

S. pombe Δyea4 disruption was done using the same methodology used to construct *Δalg5* mutants but it was generated using a disruption cassette containing the sequence of the *KanMX6* selective marker flanked by 240 bp and 299 bp of the 5' and 3' portions respectively of the *S. pombe yea4*$^+$ gene (SPBC1734.09). Primers W-c1734s: 5'-TGGAGGTTGCTGTTCAAACG-3' / X-pFA6a1-C1734a: 5'-GGGGATCCGTCGACCTGCAGCGTACGAATATCAAACCCCAAGGCCAC-3', and Y-pFA6a2-c1734: 5'-GTTTAAACGAGCTCGAATTCATCGATAGGCCCATAAGAAGTCAGTG-3´ / Z-1734a: 5'-GACCGAGCAGAAGCATATAC-3' (regions homologous to *KanMX6* are underlined) were used for the first round of PCR using *S. pombe* DNA as template. Both long primers synthesized and an excess of primers W-c1734s and Z-1734a were used in the second round of PCR to amplify the 1972 bp disruption cassette using the plasmid pFA6A-KanMX6 (Bahler *et al.*, 1998) as template. The disruption cassette was electroporated into ADpA *S. pombe* cells and geneticin resistant colonies were checked for homologous recombination using primers c1734-Xho1: 5'-ATCCGCTCGAGATGGCTGGCTTTATGCGAC-3' or SPBC1734.09fw: 5'-CTACAATATAGCAGTCGATTC-3' and KanMXrev2: 5' CGCTACCTTTGCCATGTTTCAG-3'. The resulting strain with *Δalg5::ura4*$^+$/*Δyea4::KanMX6* genotype was ADpAY-7 (Table I).

S. pombe *Δhut1* mutants were constructed as follows: A fragment (903 bp) of *hut1*$^+$ gene was obtained by PCR from genomic *S. pombe* DNA as a template using primers hut1S2: 5'-TGCATGATTGGGATTTATGG-3' and hut1Sa2: 5'-AGTATTTTGAGGCCGGCTTC-3', and ligated in vector pGEMTeasy (Promega) using manufacturer's instructions. The *Ura4*$^+$ gene was ligated in NheI site and the disruption cassette of *ura4*$^+$ gene flanked by 229 bp (5') and 670 bp (3') of *hut1*$^+$ was liberated from the construction with *EcoRI* and electroporated into Sp61A6 *S. pombe* cells. Transformants were selected in EMM lacking uracil and were checked by colony PCR using primers Hut1S1: 5'-ATCCGCTCGAGATGGCTGGCTTTATGCGAC-3' and UraAN. The resulting strain was Sp61A6H-18 (Table I).

S. pombe double, triple or quadruple mutants were obtained using standard techniques for transformation, mating, sporulation, tetrad dissection and analysis as previously described (Alfa *et al.*, 1993, D'Alessio *et al.*, 2003, Stigliano *et al.*, 2009). Spore micromanipulations were carried out with a Manual Micromanipulator (Singer Instruments Co). Relevant genotypes were determined by antibiotic resistance or prototrophy in the appropriate selective media and by colony PCR with gene-specific primers described below.

Haploid strains SpGTRK-4D and SPAC144.18-11D were obtained by inducing sporulation of the diploid heterozygous parental strains SPBPJ4664.06 and SPAC144.18 (Bioneer, Korea), respectively, upon transformation with plasmid pON177 as indicated by the company. The genotypes of the resulting Geneticine resistant haploid *Δgpt1::KanMX* and *Δvrg4::kanMX* mutants were checked by PCR using primer-pairs KanMXfw: 5'-CCTATGGAACTGCCTCGGTG-3' / GT3'NCa: 5'-GCATTGCTCACGATTAGTTG-3' and SPAC144.18fw: 5'-CCATCACGAAATTCCAAC-3' / CPN10: 5'-GATGTGAGAACTGTATCCTAGCAAG-3, respectively. A5GT-3C mutant was constructed by mating SpGTRK-4D with ADmA5.

Two different strains of *Δhut1 S. pombe* mutants were used: one set (with *ura4*$^{+}$ as a genetic marker) was constructed in this work by molecular and yeast genetic procedures described above, and the other set (with *KanMX4* as a genetic marker) was acquired from Bioneer. Double and triple mutants including *Δhut1* mutations with both genetic markers (*ura4*$^{+}$ and *KanMX4)* were constructed and used indistinctly. *Δyea4::KanMX* mutants constructed both as described above or acquired from Bioneer were used indistinctly in this work. Sp61A6HY-18 was obtained upon mating of strains Sp61A6H-18 with ADpAY. Strain SpA5HY-1D was obtained by mating strains ADpA5 and Sp61A6HY-18.

Δalg5ΔNST::kanMX double mutants A5SPAC12G12.12, A5F8.04-5d, A5SPCC1795.03-4d, A5SPBC839.11c (1C, 1A and 12A) and A5SPBC1734.09-4a were constructed by mating strain ADmA5 with the corresponding NST single mutants acquired from Bioneer. *Δalg5Δhut1ΔNST::kanMX* triple mutants A5HSPAC12G12.12-7, A5HF8.04-4 and A5HSPCC1795.03-35 were constructed by mating A5SPBC839.11c-1A double mutant with the corresponding *Δalg5ΔNST::KanMX4* double mutants. All spores resulting from sporulation of diploids obtained from the last mating were *Δalg5::ura4*$^{+}$ and *Δhut1::KanMX4,* and the mutation of the other corresponding NST was verified by PCR using NST gene-specific primers. Construction of A5H83.11-2A and A583.11-1D triple and double mutants was done by mating SPBC83.11 with SPBC839.11-12A and construction of A5H22E12-5C and A522E12-4B triple and double mutants was done by mating SP22E12.01 with SPBC839.11-1A. Quadruple mutant SpA5HYSPAC12G12.12-19C was constructed by mating strains ADpA5HY-1D and A5SPAC12G12.12, identifying resulting spores unable to grow at 35°C (*Δalg5Δhut1*) and G418 resistant, that were positive by PCR for both *Δyea4* and *Δgms2* mutant genotypes.

The following primers were used to check the genotypes of *ΔNST::KanMX4* strains not described before: for *Δgms1::kanMX4*, kanMXfw and SPCC1795.03rev: 5'-

ATCAAGCCTGTTCTATCACG-3'; for *Δgms2::KanMX4,* SPAC12G12.12fw: 5'-GATACTCTCGACATTTAC-3' and CPN10; for *Δpet1::KanMX4,* SPAC22F8.04fw: 5'-CTTCTTCACGCCTCTAATAC-3' and CPN10; for *Δpet2::KanMX4,* SPBC83.11fw: 5'-TTATGTGGTGTTAGCGAAGG-3' and KanMXrev2; for *Δpet3::KanMX4,* SPAC22E12.01fw: 5'-TTTGTAGAGTTTTATGCTAG-3' and CPN10; for *Δhut1::KanMX4,* SPBC839.11fw: 5'-GACCCTTTTTGCTTTATCC-3' and CPN10.

Construction of S. cerevisiae NST mutants and expression of S. pombe UGGT

S. cerevisiae strains employed are indicated in Table III. Strain ASGII-16 was obtained by mating PRY225-3 (Abeijon *et al.*, 1993) with RSY263 (Kaiser & Schekman, 1990) in YPDA and selecting the appropriate genetic markers as described (D'Alessio *et al.*, 2005). Strains AH-7D and AY4-5A were constructed by mating ASGII-16D with YPL244c and YEL004w, respectively. Diploid cultures were sporulated in 0.3% potassium acetate and resulting asci were digested with 1 mg/ml Zymolyase 100T and dissected in YPDA with a manual micromanipulator. Spores were germinated at 24 °C and replica-plated to different solid media to be analyzed for relevant auxotrophic markers, G418 resistance, and temperature sensitivity at 37 °C. Ura^- mutants were chosen in all cases and further transformed with p416 (URA3)-*gpt1*$^+$ as described (D'Alessio *et al.*, 2005).

Growth rate and cell morphology phenotypes of S. pombe NST mutants

Liquid cultures of *S. pombe* strains to be analyzed were grown in YES to an OD_{600}=1. An aliquot of each mutant culture was taken and photographed with a Zeiss Axio Imager 2 microscope using an *EC Plan-Neofluar 100x*/1.30 Oil objective. One-tenth serial dilutions were then performed in YES with the remaining culture and a drop of 5 µl of each dilution was plated in solid YES. The plates were incubated at 28°C or 35°C for up to 5 days to analyze growth rate and thermal sensitivity.

Subcellular fractionation

Preparation of purified ER vesicles of *S. pombe* mutants was performed as described before (D'Alessio *et al.*, 2003) with the following modifications: 3 liters of exponentially growing yeast cultures grown in rich YES media were harvested, washed, converted to spheroplasts and broken as described (D'Alessio *et al.*, 2003). The post-nuclear supernatant was centrifuged for 8 min at 5,000 x *g* and the pellet resuspended in 1.5 ml of membrane buffer (10 mM TEA/acetic acid pH 7.2, 1 mM EDTA) containing 0.8 M sorbitol and 10 µM leupeptin, 1 µM pepstatin, 1 mM phenylmethylsulfonyl fluoride, 1 mM tosylphenylalanyl chloromethylketone, 1µM E-64, and 0.5 mM tosyl-lysine chloromethyl ketone. Membranes were poured onto a discontinuous density gradient formed by 11 ml layers of 26, 40, and 50% (w/w) sucrose concentrations in membrane buffer with 5 mM $MgCl_2$ and then centrifuged for 3 h at 28,000 rpm in a SW28 rotor. ER and Golgi fractions were collected from the 40-50 % and the 26-40 % interphases, respectively, diluted 5-fold in membrane buffer plus 0.8 M sorbitol plus protease inhibitors and centrifuged for 45 min at 170,000 x *g*. The pellets were resuspended in 400 µl of the last buffer, homogenized with three strokes in a Potter-Elvehjem homogenizer and aliquots frozen in liquid N_2. Protein concentrations of the ER preparations were measured by a Bio-Rad Protein Assay as described by the manufacturer. Purity of the fractions was verified measuring glucosidase II (ER marker) and galactosytransferase (Golgi marker) activities as described (D'Alessio *et al.*, 2003). Integrity of the vesicles was determined by comparing the activity of the fractions with and without the addition of the detergent digitonin. Latency was over 95% in all cases.

UDP-Glc transport assays

Uptake of UDP-[^{3}H]Glc into ER vesicles was measured by the ultracentrifugation method in duplicates in 1 ml of transport buffer (0.5 M sucrose, 30 mM TEA/acetic acid pH 7.2, 5 mM $MgCl_2$, and 5 mM $MnCl_2$) containing 0.5 mg of protein ER membranes and 2 µM UDP-Glc for 5 min at 0 ^{0}C or 30 ^{0}C as described (Berninsone *et al.*, 2001). The reactions were stopped with 3

ml stop buffer (1 M sucrose, 1 mM EDTA) and the vesicles were ultracentrifuged. The pellets were then resuspended in 4 ml of stop buffer and ultracentrifuged four more times. The vesicles were then lysed upon incubation in 1 ml 4% perchloric acid for 30 min, centrifuged, and label in the supernatants was quantified. Transport of UDP-[^{14}C]Glc into ER vesicles was measured by the filtration method in duplicates in 1 ml of SHM buffer (0.25 M sucrose, 10 mM HEPES buffer pH 7.5 and 1 mM $MgCl_2$) containing 100 µg of protein corresponding to the ER vesicles and 1 µM UDP-[^{14}C]Glc (0.1 µCi) for 5 min at 0 ^{0}C or 30 °C as described (Blanco-Herrera *et al.*, 2015). The vesicles were diluted in cold SHM buffer and filtered through 0.45-µm cellulose ester filters (Millipore). The filters were washed with 10 volumes of cold SHM buffer and dried. The radioactivity on the filters was determined by liquid scintillation counting. Radioactivity detected in the filters of the reactions performed at 0 °C was subtracted from the values obtained at 30 °C.

Analysis of glycans synthesized in vivo

Labeling of cells and isolation of Endo H-sensitive glycans was performed as described before except that cells were pre-incubated for 60 min with 5 mM NMDNJ, 8 mM CST and for 5 min with 5 mM DTT before addition of the labeled precursor (Stigliano *et al.*, 2011). As already reported, *N*-glycans were first run on paper chromatography, eluted and then resolved by HPLC (Stigliano *et al.*, 2011).

Analysis of cell wall and glycan monosaccharide components

Cells (200 mg, wet weight) were incubated for 60 min at 25 ^{0}C in 0.55 ml of 1 % YNB, 5 mM Glc plus 200 µCi [^{14}C]Glc (300 Ci/M) after which 50 ml of 1 M Glc were added and cells further incubated for 120 min. Cells were then processed as indicated above (analysis of glycans synthesized *in vivo*). The pellets obtained after extensive proteolytic degradation were washed twice with 1 ml water and heated at 100 ^{0}C for 120 min in 2 N NaOH. Two volumes of methanol

were then added and the precipitates thus obtained were resuspended in 1 ml water and re-precipitated with two volumes of methanol three times. The precipitates were then heated for 240 min in 0.5 ml 1 N HCl, dried at room temperature and run on Whatman 1 papers with 1-butanol/pyridine/water (10:3:3) as solvent. Acid hydrolysis and analysis of Endo H-sensitive *N*-glycan monosaccharide components was similarly performed.

ACKNOWLEDGEMENTS

We thank Susana Raffo for the synthesis of UDP-[^{14}C]Glc and Dr. C. Abeijon and R. Shekman for strains PRY225-3 and RSY263, respectively. This work was supported by the National Research Council (CONICET, Argentina) [Grant PIP-11220090100811]. L.M.B, C.M.B, A.J.P., and C.D. are Career Investigators of the National Research Council (CONICET, Argentina).

ABBREVIATIONS

† The abbreviations used are: ER, endoplasmic reticulum; Endo H, endo-β-*N*-acetylglucosaminidase H; UGGT, UDP-Glc:glycoprotein glucosyltransferase; NS, nucleotide sugar; NST, nucleotide sugar transporter

REFERENCES

Abeijon C, Yanagisawa K, Mandon EC, Hausler A, Moremen K, Hirschberg CB, Robbins PW. 1993. Guanosine diphosphatase is required for protein and sphingolipid glycosylation in the Golgi lumen of *Saccharomyces cerevisiae*. *J Cell Biol.* 122:307-323.

Alfa C, Fantes P, Hyams J, McLeod M, Wabrik E. 1993. Experiments with Fission Yeast: A Laboratory Manual. *Cold Spring Harbor, NY: Cold Spring Harbor Laboratory Press.*

Altschul SF, Gish W, Miller W, Myers EW, Lipman DJ. 1990. Basic local alignment search tool. *J Mol Biol.* 215:403-410.

Atkinson HJ, Morris JH, Ferrin TE, Babbitt PC. 2009. Using sequence similarity networks for visualization of relationships across diverse protein superfamilies. *PLoS One.* 4:e4345.

Bahler J, Wu JQ, Longtine MS, Shah NG, McKenzie A, 3rd, Steever AB, Wach A, Philippsen P, Pringle JR. 1998. Heterologous modules for efficient and versatile PCR-based gene targeting in *Schizosaccharomyces pombe*. *Yeast.* 14:943-951.

Berninsone P, Miret JJ, Hirschberg CB. 1994. The Golgi guanosine diphosphatase is required for transport of GDP-mannose into the lumen of *Saccharomyces cerevisiae* Golgi vesicles. *J Biol Chem.* 269:207-211.

Berninsone P, Hwang HY, Zemtseva I, Horvitz HR, Hirschberg CB. 2001. SQV-7, a protein involved in *Caenorhabditis elegans* epithelial invagination and early embryogenesis, transports UDP-glucuronic acid, UDP-N- acetylgalactosamine, and UDP-galactose. *Proc Natl Acad Sci U S A.* 98:3738-3743.

Blanco-Herrera F, Moreno AA, Tapia R, Reyes F, Araya M, D'Alessio C, Parodi A, Orellana A. 2015. The UDP-glucose: glycoprotein glucosyltransferase (UGGT), a key enzyme in ER quality control, plays a significant role in plant growth as well as biotic and abiotic stress in *Arabidopsis thaliana*. *BMC Plant Biol.* 15:127.

Braakman I, Helenius J, Helenius A. 1992. Manipulating disulfide bond formation and protein folding in the endoplasmic reticulum. *EMBO J.* 11:1717-1722.

Caffaro CE, Hirschberg CB, Berninsone PM. 2006. Independent and simultaneous translocation of two substrates by a nucleotide sugar transporter. *Proc Natl Acad Sci U S A.* 103:16176-16181.

Caffaro CE, Luhn K, Bakker H, Vestweber D, Samuelson J, Berninsone P, Hirschberg CB. 2008. A single *Caenorhabditis elegans* Golgi apparatus-type transporter of UDP-glucose, UDP-galactose, UDP-*N*-acetylglucosamine, and UDP-*N*-acetylgalactosamine. *Biochemistry.* 47:4337-4344.

Castro O, Chen LY, Parodi AJ, Abeijon C. 1999. Uridine diphosphate-glucose transport into the endoplasmic reticulum of *Saccharomyces cerevisiae*: *in vivo* and *in vitro* evidence. *Mol Biol Cell.* 10:1019-1030.

D'Alessio C, Trombetta ES, Parodi AJ. 2003. Nucleoside diphosphatase and glycosyltransferase activities can localize to different subcellular compartments in *Schizosaccharomyces pombe*. *J Biol Chem.* 278:22379-22387.

D'Alessio C, Caramelo JJ, Parodi AJ. 2005. Absence of nucleoside diphosphatase activities in the yeast secretory pathway does not abolish nucleotide sugar-dependent protein glycosylation. *J Biol Chem.* 280:40417-40427.

D'Alessio C, Caramelo JJ, Parodi AJ. 2010. UDP-GlC:glycoprotein glucosyltransferase-glucosidase II, the ying-yang of the ER quality control. *Semin Cell Dev Biol.* 21:491-499.

Dean N, Zhang YB, Poster JB. 1997. The VRG4 gene is required for GDP-mannose transport into the lumen of the Golgi in the yeast *Saccharomyces cerevisiae*. *J Biol Chem.* 272:31908-31914.

Fanchiotti S, Fernandez F, D'Alessio C, Parodi AJ. 1998. The UDP-Glc:Glycoprotein glucosyltransferase is essential for *Schizosaccharomyces pombe* viability under conditions of extreme endoplasmic reticulum stress. *J Cell Biol.* 143:625-635.

Fernandez F, D'Alessio C, Fanchiotti S, Parodi AJ. 1998. A misfolded protein conformation is not a sufficient condition for *in vivo* glucosylation by the UDP-Glc:glycoprotein glucosyltransferase. *EMBO J.* 17:5877-5886.

Fernandez FS, Trombetta SE, Hellman U, Parodi AJ. 1994. Purification to homogeneity of UDP-glucose:glycoprotein glucosyltransferase from *Schizosaccharomyces pombe* and apparent absence of the enzyme from *Saccharomyces cerevisiae*. *J Biol Chem.* 269:30701-30706.

Finn RD, Bateman A, Clements J, Coggill P, Eberhardt RY, Eddy SR, Heger A, Hetherington K, Holm L, Mistry J*, et al.* 2014. Pfam: the protein families database. *Nucleic Acids Res.* 42:D222-230.

Finn RD, Coggill P, Eberhardt RY, Eddy SR, Mistry J, Mitchell AL, Potter SC, Punta M, Qureshi M, Sangrador-Vegas A*, et al.* 2016. The Pfam protein families database: towards a more sustainable future. *Nucleic Acids Res.* 44:D279-285.

Gao XD, Nishikawa A, Dean N. 2001. Identification of a conserved motif in the yeast golgi GDP-mannose transporter required for binding to nucleotide sugar. *J Biol Chem.* 276:4424-4432.

Hirschberg CB, Robbins PW, Abeijon C. 1998. Transporters of nucleotide sugars, ATP, and nucleotide sulfate in the endoplasmic reticulum and Golgi apparatus. *Annu Rev Biochem.* 67:49-69.

Hoffman CS, Winston F. 1987. A ten-minute DNA preparation from yeast efficiently releases autonomous plasmids for transformation of *Escherichia coli*. *Gene.* 57:267-272.

Horisberger M, Vonlanthen M, Rosset J. 1978. Localization of alpha-galactomannan and of wheat germ agglutinin receptors in *Schizosaccharomyces pombe*. *Arch Microbiol.* 119:107-111.

Jelinek-Kelly S, Akiyama T, Saunier B, Tkacz JS, Herscovics A. 1985. Characterization of a specific alpha-mannosidase involved in oligosaccharide processing in *Saccharomyces cerevisiae*. *J Biol Chem.* 260:2253-2257.

Kainuma M, Chiba Y, Takeuchi M, Jigami Y. 2001. Overexpression of HUT1 gene stimulates in vivo galactosylation by enhancing UDP-galactose transport activity in *Saccharomyces cerevisiae*. *Yeast.* 18:533-541.

Kaiser CA, Schekman R. 1990. Distinct sets of SEC genes govern transport vesicle formation and fusion early in the secretory pathway. *Cell.* 61:723-733.

Kirchberger S, Leroch M, Huynen MA, Wahl M, Neuhaus HE, Tjaden J. 2007. Molecular and biochemical analysis of the plastidic ADP-glucose transporter (ZmBT1) from Zea mays. *J Biol Chem.* 282:22481-22491.

Krawchuk MD, Wahls WP. 1999. High-efficiency gene targeting in *Schizosaccharomyces pombe* using a modular, PCR-based approach with long tracts of flanking homology. *Yeast.* 15:1419-1427.

Liu L, Xu YX, Hirschberg CB. 2010. The role of nucleotide sugar transporters in development of eukaryotes. *Semin Cell Dev Biol.* 21:600-608.

Liu L, Xu YX, Caradonna KL, Kruzel EK, Burleigh BA, Bangs JD, Hirschberg CB. 2013. Inhibition of nucleotide sugar transport in *Trypanosoma brucei* alters surface glycosylation. *J Biol Chem.* 288:10599-10615.

Martin-Garcia R, Duran A, Valdivieso MH. 2003. In *Schizosaccharomyces pombe* chs2p has no chitin synthase activity but is related to septum formation. *FEBS Lett.* 549:176-180.

Matsuyama A, Arai R, Yashiroda Y, Shirai A, Kamata A, Sekido S, Kobayashi Y, Hashimoto A, Hamamoto M, Hiraoka Y*, et al.* 2006. ORFeome cloning and global analysis of protein localization in the fission yeast *Schizosaccharomyces pombe*. *Nat Biotechnol.* 24:841-847.

Milla ME, Hirschberg CB. 1989. Reconstitution of Golgi vesicle CMP-sialic acid and adenosine 3'-phosphate 5'-phosphosulfate transport into proteoliposomes. *Proc Natl Acad Sci U S A.* 86:1786-1790.

Moreno S, Klar A, Nurse P. 1991. Molecular genetic analysis of fission yeast *Schizosaccharomyces pombe*. *Methods Enzymol.* 194:795-823.

Movsichoff F, Castro OA, Parodi AJ. 2005. Characterization of *Schizosaccharomyces pombe* ER alpha-mannosidase: a reevaluation of the role of the enzyme on ER-associated degradation. *Mol Biol Cell.* 16:4714-4724.

Nakanishi H, Nakayama K, Yokota A, Tachikawa H, Takahashi N, Jigami Y. 2001. Hut1 proteins identified in *Saccharomyces cerevisiae* and *Schizosaccharomyces pombe* are functional homologues involved in the protein-folding process at the endoplasmic reticulum. *Yeast.* 18:543-554.

Nishikawa A, Mendez B, Jigami Y, Dean N. 2002. Identification of a *Candida glabrata* homologue of the *S. cerevisiae* VRG4 gene, encoding the Golgi GDP-mannose transporter. *Yeast.* 19:691-698.

Norambuena L, Marchant L, Berninsone P, Hirschberg CB, Silva H, Orellana A. 2002. Transport of UDP-galactose in plants. Identification and functional characterization of AtUTr1, an *Arabidopsis thaliana* UDP-galactos/UDP-glucose transporter. *J Biol Chem.* 277:32923-32929.

Notredame C, Higgins DG, Heringa J. 2000. T-Coffee: A novel method for fast and accurate multiple sequence alignment. *J Mol Biol.* 302:205-217.

Ohashi T, Takegawa K. 2010. N- and O-linked oligosaccharides completely lack galactose residues in the gms1och1 mutant of *Schizosaccharomyces pombe*. *Appl Microbiol Biotechnol.* 86:263-272.

R Core Team. 2013. R: A language and environment for statistical computing R Foundation for Statistical Computing. http://www.R-project.org/

Reyes F, Leon G, Donoso M, Brandizzi F, Weber AP, Orellana A. 2010. The nucleotide sugar transporters AtUTr1 and AtUTr3 are required for the incorporation of UDP-glucose into the endoplasmic reticulum, are essential for pollen development and are needed for embryo sac progress in *Arabidopsis thaliana*. *Plant J.* 61:423-435.

Roy SK, Chiba Y, Takeuchi M, Jigami Y. 2000. Characterization of Yeast Yea4p, a uridine diphosphate-*N*-acetylglucosamine transporter localized in the endoplasmic reticulum and required for chitin synthesis. *J Biol Chem.* 275:13580-13587.

Sambrook J, Russell DW. 2001. *Molecular cloning: a laboratory manual*. Cold Spring Harbor, NY: Cold Spring Harbor Laboratory Press.

Segawa H, Ishida N, Takegawa K, Kawakita M. 1999. *Schizosaccharomyces pombe* UDP-galactose transporter: identification of its functional form through cDNA cloning and expression in mammalian cells. *FEBS Lett.* 451:295-298.

Seino J, Ishii K, Nakano T, Ishida N, Tsujimoto M, Hashimoto Y, Takashima S. 2010. Characterization of rice nucleotide sugar transporters capable of transporting UDP-galactose and UDP-glucose. *J Biochem.* 148:35-46.

Shannon PT, Grimes M, Kutlu B, Bot JJ, Galas DJ. 2013. RCytoscape: tools for exploratory network analysis. *BMC Bioinformatics.* 14:217.

Soliman A, Ayele BT, Daayf F. 2014. Biochemical and molecular characterization of barley plastidial ADP-glucose transporter (HvBT1). *PLoS One.* 9:e98524.

Stigliano ID, Caramelo JJ, Labriola CA, Parodi AJ, D'Alessio C. 2009. Glucosidase II Beta Subunit Modulates *N*-Glycan Trimming in Fission Yeasts and Mammals. *Mol Biol Cell.* 20:3974-3984.

Stigliano ID, Alculumbre SG, Labriola CA, Parodi AJ, D'Alessio C. 2011. Glucosidase II and *N*-glycan mannose content regulate the half-lives of monoglucosylated species *in vivo*. *Mol Biol Cell.* 22:1810-1823.

Tanaka N, Takegawa K. 2001. Functional characterization of Gms1p/UDP-galactose transporter in *Schizosaccharomyces pombe*. *Yeast.* 18:745-757.

Trombetta ES, Helenius A. 1999. Glycoprotein reglucosylation and nucleotide sugar utilization in the secretory pathway: identification of a nucleoside diphosphatase in the endoplasmic reticulum. *EMBO J.* 18:3282-3292.

UniProt Consortium. 2015. UniProt: a hub for protein information. *Nucleic Acids Res.* 43:D204-212.

Wright A, Robbins PW. 1965. The enzymatic synthesis of uridine diphosphate [^{14}C]glucose. *Biochim Biophys Acta.* 104:594-595.

Yoritsune K, Higuchi Y, Matsuzawa T, Takegawa K. 2014. Functional analysis of putative phosphoenolpyruvate transporters localized to the Golgi apparatus in *Schizosaccharomyces pombe*. *FEMS Yeast Res.* 14:1101-1109.

LEGENDS TO FIGURES

Figure 1. Characterization of *S. pombe Δvrg4* mutants. *A,B*, monosaccharide composition of wild type and *Δvrg4* mutant cell walls. Cell walls of indicated strains were submitted to strong acid hydrolysis. Resulting monosaccharides were run on paper chromatography with 1-butanol/pyridine/water (10:3:3) as solvent. Position of standards is indicated. *C,D*, phenotype of *S. pombe ⊿vrg4* mutants. Liquid cultures of *S. pombe* wild type and *Δvrg4* mutant strains were grown in YES to an OD_{600} of 1. *C*, one-tenth serial dilutions were performed in YES and a drop of 5 µl of each dilution was plated in solid YES and incubated at 28°C or 35°C for the indicated times. *D*, live cells were photographed using a Zeiss Axio Imager 2 microscope with an *EC Plan-Neofluar 100x*/1.30 Oil objective. Bar= 10 µm.

Figure 2. Similarity network of genes of known specificity and *S. pombe* genes. Thresholded sequence similarity networks represent sequences as nodes (filled circles) and all pairwise sequence relationships (alignments) better than a bit score BLAST threshold (indicated in each panel) as edges (lines). *A*, E-value threshold = 10 (all nodes are linked); *B*, E-value threshold = $1x10^{-10}$; *C*, E-value threshold = $1x10^{-20}$; *D*, E-value threshold = $1x10^{-25}$ and *E*, E-value threshold = $1x10^{-35}$. Filled circles correspond to Pfam families PF08449 (violet); PF03151 (yellow); PF04142 (red) and PF00153 (pink). No Pfam family assigned was indicated with white filled circles and filled green ones were used to label S. *pombe* putative transporters. The relative positioning of disconnected groups has no meaning, while the lengths of connecting edges correlate with the relative dissimilarities of each pair of sequences. Color stars indicate the NS transported.

Figure 3. **Growth of *S. pombe* mutants at 28 ^{0}C and 35 ^{0}C**. Liquid cultures of indicated *S. pombe* strains were grown in YES to an OD_{600} of 1. One-tenth serial dilutions were performed in YES and a drop of 5 µl of each dilution was plated in solid YES and incubated at 28°C or 35°C for the indicated times.

Figure 4. Morphology of wild type and *S. pombe* mutants. Liquid cultures of indicated *S. pombe* strains were grown in YES to an OD600 of 1. Live cells were photographed using a Zeiss Axio Imager 2 microscope with an *EC Plan-Neofluar 100x*/1.30 Oil objective. Bar= 10 µm. Panel A (*WT*) is the same figure as Panel *D* in Figure 1

Figure 5. UDP-Glc entrance into *S. pombe* ER-derived vesicles. Uptake of radiolabeled UDP-Glc into ER-derived vesicles at 30 °C for 5 min was measured by the centrifugation (*A*) or filtration (*B*) methods. Uptake at 0°C was subtracted from data obtained for each strain ER-derived membranes. *Δalg5Δhut1Δyea4* and *Δalg6Δhut1* mutants were compared with parental strains *Δalg5* (*A*) or *Δalg6* (*B*). Results are the average of duplicate experiments.

Figure 6. *N*-glycans synthesized by *S. pombe* and *S. cerevisiae* double mutants. *N*-glycan patterns synthesized by *S. pombe Δalg5* (*A*), *Δalg5Δgpt1* (*B*), *Δalg5Δhut*1 *(C*) *Δalg5Δyea4* (*E*), or *S. cerevisiae* (expressing *S. pombe* UGGT) *Δalg5Δhut1* (*D*) and *Δalg5Δyea4* (*F*) mutants. Cells were labeled *in vivo* with [^{14}C]-Glc and EndoH-sensitive *N*-glycans were first run on paper chromatography, eluted and further resolved by HPLC. Position of standards is indicated.

Figure 7. *N*-glycans synthesized by *S. pombe* triple and quadruple mutants. Endo H-sensitive *N*-glycans synthesized by indicated *S. pombe* triple or quadruple mutants were first run on paper chromatography and further resolved by HPLC. Position of standards is indicated.

Figure 8. Monosaccharide composition of *N*-glycans. Endo H-sensitive *N*-glycans synthesized by indicated *S. pombe* (*A, C, E-J*) or *S. cerevisiae* (*B, D,* expressing *S. pombe* UGGT) strains were submitted to strong acid hydrolysis and run on paper chromatography with 1-butanol/pyridine/water (10:3:3) as solvent. Position of the standards is indicated.

.

Table I. *S. pombe* strains used in this study.

Strain (nickname)	Genotype	Source
ADm (WT)	*h⁻, leu1-32, ade6-M210, ura4-D18*	Our stock
ADp (WT)	*h⁺, leu1-32, ade6-M216, ura4-D18*	Our stock
SPAC12G12.12 *(Δgms2)*	*h⁺, leu1-32, ade6-M216, ura4-D18, Δgms2::KanMX4*	Bioneer
SPAC22F8.04 *(Δpet1)*	*h⁺, leu1-32, ade6-M216, ura4-D18, Δpet1::KanMX4*	Bioneer
SPCC1795.03 *(Δgms1)*	*h⁺, leu1-32, ade6-M216, ura4-D18, Δgms1::KanMX4*	Bioneer
SPBC839.11c *(Δhut1)*	*h⁺, leu1-32, ade6-M216, ura4-D18, Δhut1::KanMX4*	Bioneer
SPBC1734.09 *(Δyea4)*	*h⁺, leu1-32, ade6-M216, ura4-D18, Δyea4::KanMX4*	Bioneer
SPAC22E12.01 *(Δpet3)*	*h⁺, leu1-32, ade6-M210, ura4-D18, Δpet3::KanMX4*	Bioneer
SPBC83.11 *(Δpet2)*	*h⁺, leu1-32, ade6-M210, ura4-D18, Δpet2::KanMX4*	Bioneer
SPAC144.18 diploid *(Δvrg4/+)*	*h⁺/h⁺, leu1-32/ leu1-32, ade6-M210/ade6-M216, ura4-D18/ ura4-D18, Δvrg4::KanMX4/+*	Bioneer
SPAC144.18-11D haploid *(Δvrg4)*	*h⁺, leu1-32, ade6-M216, ura4-D18, Δvrg4::KanMX4*	This study
SPBPJ4664.06 diploid *(Δgpt1/+)*	*h⁺/h⁺, leu1-32/ leu1-32, ade6-M210/ade6-M216, ura4-D18/ ura4-D18, Δgpt1::KanMX4/+*	Bioneer
SpGTRK-4D haploid *(Δgpt1)*	*h⁺, leu1-32, ade6-M216, ura4-D18, Δgpt1:: KanMX4*	This study
ADpA5 *(Δalg5)*	*h⁺, leu1-32, ade6-M216, ura4-D18, Δalg5::ura4⁺*	This study
ADmA5 *(Δalg5)*	*h⁻, leu1-32, ade6-M210, ura4-D18, Δalg5::ura4⁺*	This study
ADpA *(Δalg6)*	*h⁺, leu1-32, ade6-M216, ura4-D18, Δalg6:: ura4⁺*	This study
Sp61A *(Δalg6)*	*h⁻, leu1-32, ade1, ade6-M210, ura4-D18, Δalg6:: ura4⁺*	Our stock
Sp61A6 *(Δalg6::Δura4)*	*h⁻, leu1-32, ade1, ade6-M210, ura4-D18, Δalg6::Δura4*	This study
Sp61A6H-18 *(Δalg6/Δhut1)*	*h⁻, leu1-32, ade1, ade6-M210, ura4-D18, Δalg6::Δura4, Δhut1::ura4⁺*	This study
ADpAY-7 *(Δalg6/Δyea4)*	*h⁺, leu1-32, ade6-M216, ura4-D18, Δalg6::ura4⁺, Δyea4::KanMX6*	This study
Sp61A6HY-18 *(Δalg6/Δhut1/Δyea4)*	*h⁻, leu1-32, ade6-M210, ura4-D18, Δalg6::Δura4, Δhut1::ura4⁺, Δyea4::KanMX6*	This study
ADpA5HY-1D *(Δalg5/Δhut1/Δyea4)*	*h⁺, leu1-32, ade6-M210, ura4-D18, Δalg5::ura4⁺, Δhut1::ura4⁺, Δyea4::KanMX6*	This study
A5GT-3C *(Δalg5/Δgpt1)*	*h⁻, leu1-32, ade6-M210, ura4-D18, Δalg5::ura4⁺, Δgpt1::KanMX4*	This study
A5SPAC12G12.12 *(Δalg5/Δgms2)*	*h⁺, leu1-32, ade6-M216, ura4-D18, Δalg5::ura4⁺, Δgms2::KanMX4*	This study
A5F8.04 5d *(Δalg5/Δpet1)*	*h⁺, leu1-32, ade6-M216, ura4-D18, Δalg5::ura4⁺, Δpet1::KanMX4*	This study
A5SPCC1795.03-4d *(Δalg5/Δgms1)*	*h⁺, leu1-32, ade6-M216, ura4-D18, Δalg5::ura4⁺, Δgms1::KanMX4*	This study
A5SPBC839.11c-1C *(Δalg5/Δhut1 1C)*	*h⁺, leu1-32, ade6-M216, ura4-D18, Δalg5::ura4⁺, Δhut1::KanMX4*	This study
A5SPBC839.11c-1A *(Δalg5/Δhut1 1A)*	*h⁻, leu1-32, ade6-M210, ura4-D18, Δalg5::ura4⁺, Δhut1::KanMX4*	This study
A5SPBC839.11c-12A *(Δalg5/Δhut1 12A)*	*h⁻, leu1-32, ade6-M216, ura4-D18, Δalg5::ura4⁺, Δhut1::KanMX4*	This study
A5SPBC1734.09-4A *(Δalg5/Δyea4)*	*h⁺, leu1-32, ade6-M216, ura4-D18, Δalg5::ura4⁺, Δyea4::KanMX4*	This study
A583.11-1D *(Δalg5/Δpet2)*	*h⁻, leu1-32, ade6-M210, ura4-D18, Δalg5::ura4⁺,Δpet2::KanMX4*	This study
A522E12-4B *(Δalg5/Δpet3)*	*h⁻, leu1-32, ade6-M210, ura4-D18, Δalg5::ura4⁺,Δpet3::KanMX4*	This study
A5HSPAC12G12.12-7 *(Δalg5/Δhut1/Δgms2)*	*h⁻, leu1-32, ade6-M210, ura4-D18, Δalg5::ura4⁺, Δhut1::KanMX4, Δgms2::KanMX4*	This study
A5HF8.04-4 *(Δalg5/Δhut1/Δpet1)*	*h⁻, leu1-32, ade6-M210, ura4-D18, Δalg5::ura4⁺, Δhut1::KanMX4, Δpet1::KanMX4*	This study
A5HSPCC1795.03-35 *(Δalg5/Δhut1/Δgms1)*	*h⁺, leu1-32, ade6-M216, ura4-D18, Δalg5::ura4⁺, Δhut1::KanMX4, Δgms1::KanMX4*	This study
A5H83.11-2A *(Δalg5/Δhut1/Δpet2)*	*h⁺, leu1-32, ade6-M210, ura4-D18, Δalg5::ura4⁺,Δhut1::KanMX4, Δpet2::KanMX4*	This study
A5H22E12-5C *(Δalg5/Δhut1/Δpet3)*	*h⁻, leu1-32, ade6-M210, ura4-D18, Δalg5::ura4⁺,Δhut1::KanMX4, Δpet3::KanMX4*	This study
A5HYSPAC12G12.12-19C *(Δalg5/Δhut1/Δyea4/Δgms2)*	*h⁺, leu1-32, ade6-M216, ura4-D18, Δalg5::ura4⁺, Δhut1::ura4⁺, Δyea4::KanMX6, Δgms2::KanMX4*	This study

Table II. *S. cerevisiae* strains used in this study.

Strains (nickname)	**Genotype**	**Source**
YPL244c *(Δhut1)*	*MATα, his3Δ1, leu2Δ0, lys2Δ0, ura3Δ0, ΔYPL244c::kanMX4*	Euroscarf
YEL004w *(Δyea4)*	*MATα, his3Δ1, leu2Δ0, lys2Δ0, ura3Δ0, ΔYEL004w::kanMX4*	Euroscarf
PRY225-3	*MATa, Δynd1::kanMX4, Δalg5::HIS3, Δgls2::URA3, ura3-52, lys2, ade2, his3, trp1, leu2*	(Abeijon *et al.*, 1993)
RSY263	*MATα, sec12-4, ura3-52, his4*	(Kaiser & Schekman, 1990)
ASGII-16D	*MATa, Δalg5::HIS3, Δgls2::URA3, ura3-52, sec12-4, ura3-52, lys2, leu2*	This study
AH-7D (*Δalg5/Δhut1*)	*MATα, Δalg5::HIS3, ΔYEL004w::kanMX4, ura3-52, lys2, ade2, leu2*	This study
AY4-5A (*Δalg5/Δyea4*)	*MATα, Δalg5::HIS3, ΔYPL244c::kanMX4,*	This study

Table III: *S. pombe* genes belonging to the three Pfam families of NSTs of experimentally characterized specificity of the secretory pathway.

Pfam family	UniProt accession	Gene name	Refseq accession	Systematic ID	Localization
PF08449 UAA family	HUT1_SCHPO	*hut1*$^{+}$	NP_595251	SPBC839.11c	ER (Matsuyama *et al.*, 2006)
	GMT_SCHPO	*vrg4*$^{+}$	NP_594679	SPAC144.18	ND
	YEA4_SCHPO	*yea4*$^{+}$	NP_595426	SPBC1734.09	ER/ cell tip (Matsuyama *et al.*, 2006)
PF04142 NST family	GMS1_SCHPO	*gms1*$^{+}$	NP_588041	SPCC1795.03	Golgi (Tanaka & Takegawa, 2001)
	YAGC_SCHPO	*gms2*$^{+}$	NP_592886	SPAC12G12.12	ND
PF03151 TPT family	YIY4_SCHPO	*pet1*$^{+}$	NP_594727	SPAC22F8.04	Golgi (Matsuyama *et al.*, 2006, Yoritsune *et al.*, 2014)
	YG1B_SCHPO	*pet2*$^{+}$	NP_595643	SPBC83.11	Golgi (Yoritsune *et al.*, 2014)
	YDB1_SCHPO	*pet3*$^{+}$	NP_594827	SPAC22E12.01	Golgi (Matsuyama *et al.*, 2006)

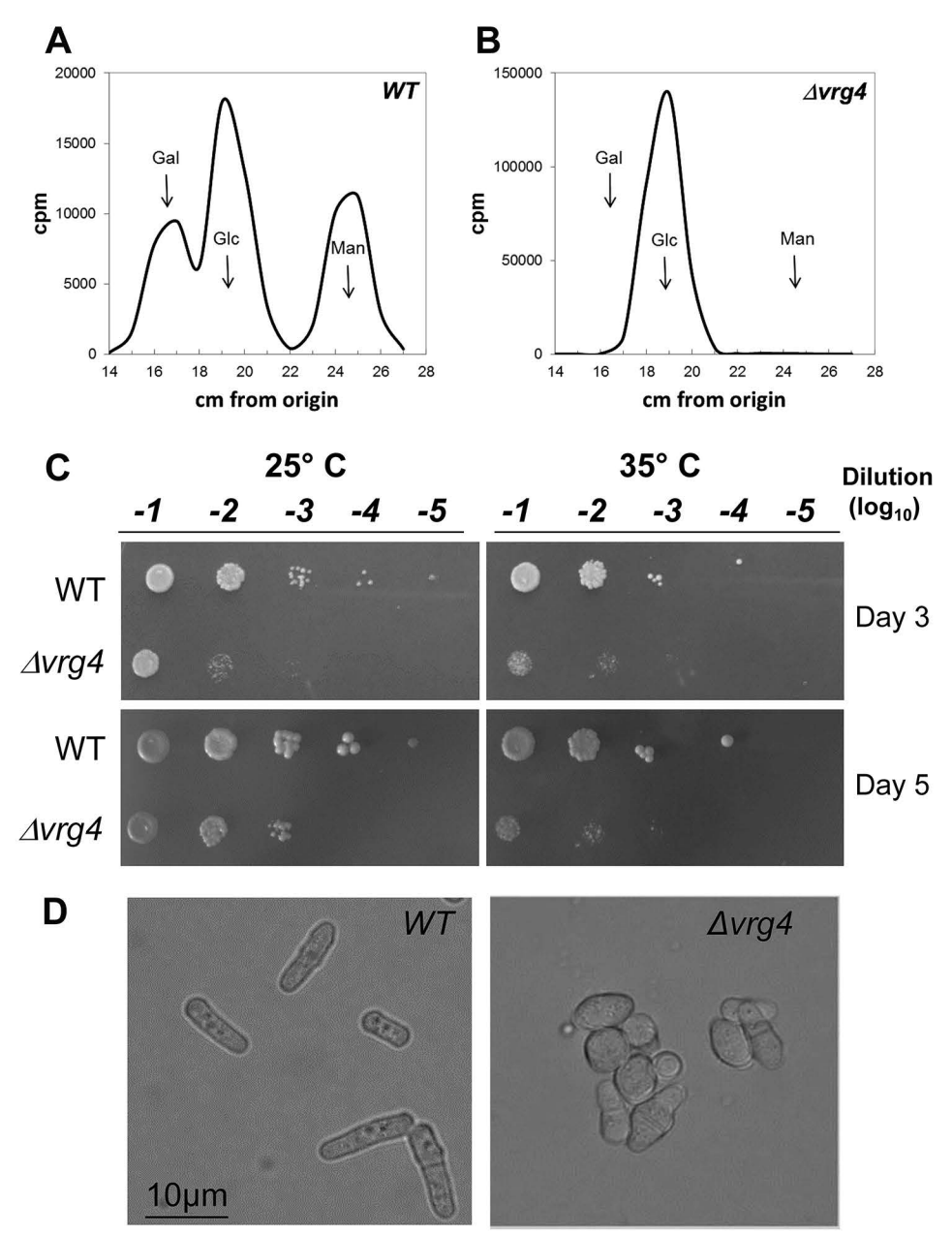
A
WT
cpm
20000
15000
10000
5000
0
Gal
Glc
Man
14
16
18
20
22
24
26
28
cm from origin
B
Δvrg4
cpm
150000
100000
50000
0
Gal
Glc
Man
14
16
18
20
22
24
26
28
cm from origin
C
25° C
35° C
Dilution (log10)
-1
-2
-3
-4
-5
WT
Δvrg4
Day 3
Day 5
D
WT
Δvrg4
10μm

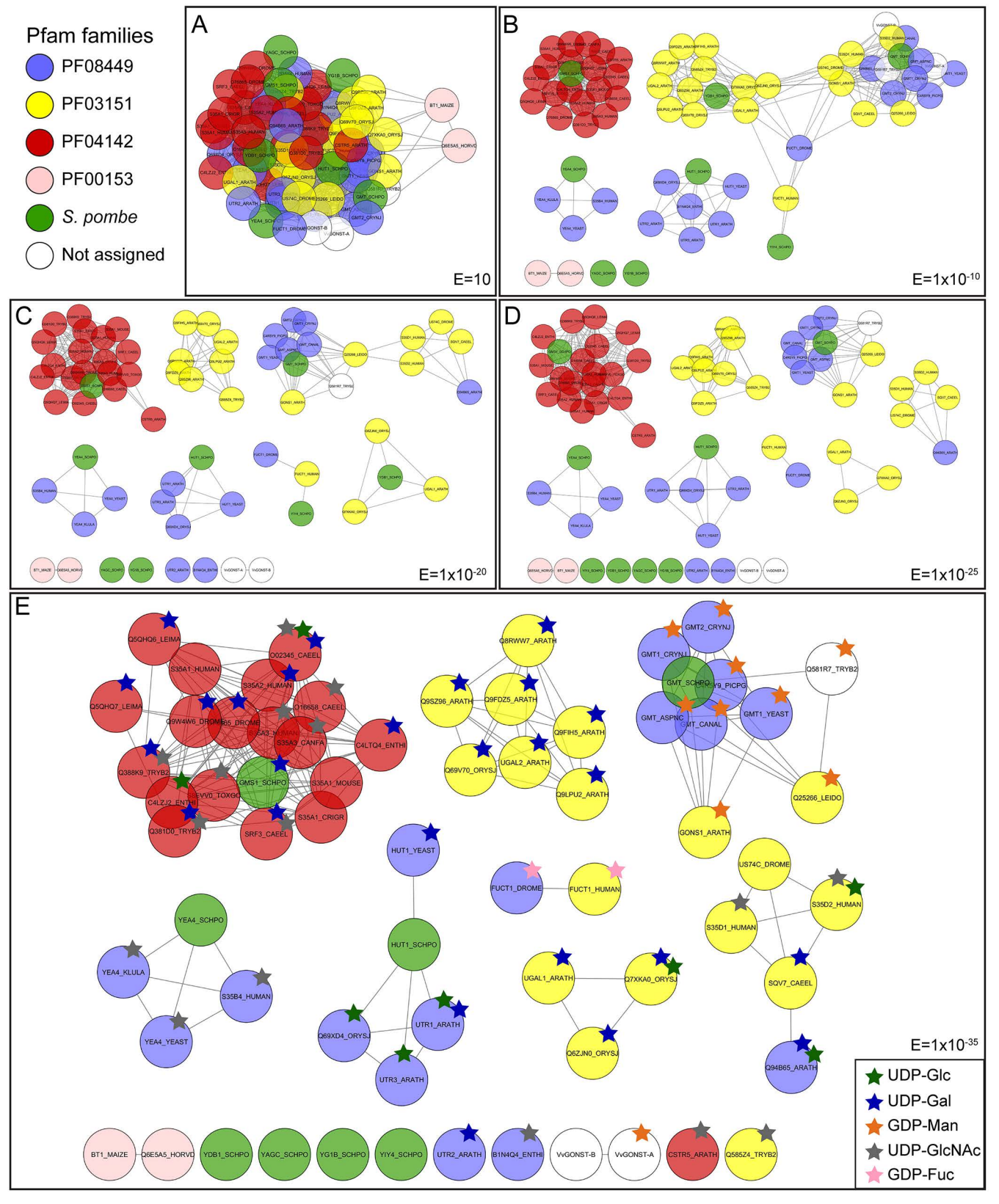
Pfam families
PF08449
PF03151
PF04142
PF00153
S. pombe
Not assigned
A
E=10
B
E=1x10-10
C
E=1x10-20
D
E=1x10-25
E
E=1x10-35
UDP-Glc
UDP-Gal
GDP-Man
UDP-GlcNAc
GDP-Fuc

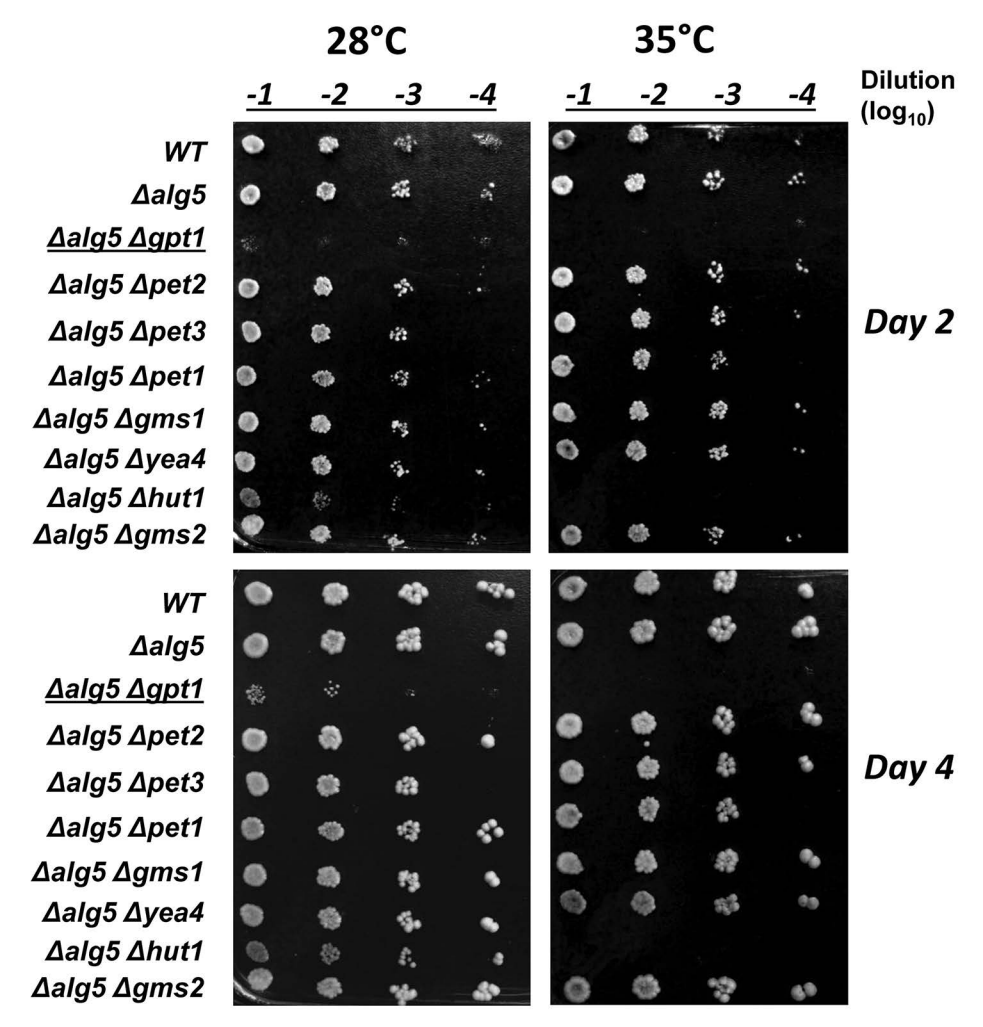
28°C
35°C
-1
-2
-3
-4
-1
-2
-3
-4
Dilution (log10)
WT
Δalg5
Δalg5 Δgpt1
Δalg5 Δpet2
Δalg5 Δpet3
Δalg5 Δpet1
Δalg5 Δgms1
Δalg5 Δyea4
Δalg5 Δhut1
Δalg5 Δgms2
Day 2
WT
Δalg5
Δalg5 Δgpt1
Δalg5 Δpet2
Δalg5 Δpet3
Δalg5 Δpet1
Δalg5 Δgms1
Δalg5 Δyea4
Δalg5 Δhut1
Δalg5 Δgms2
Day 4

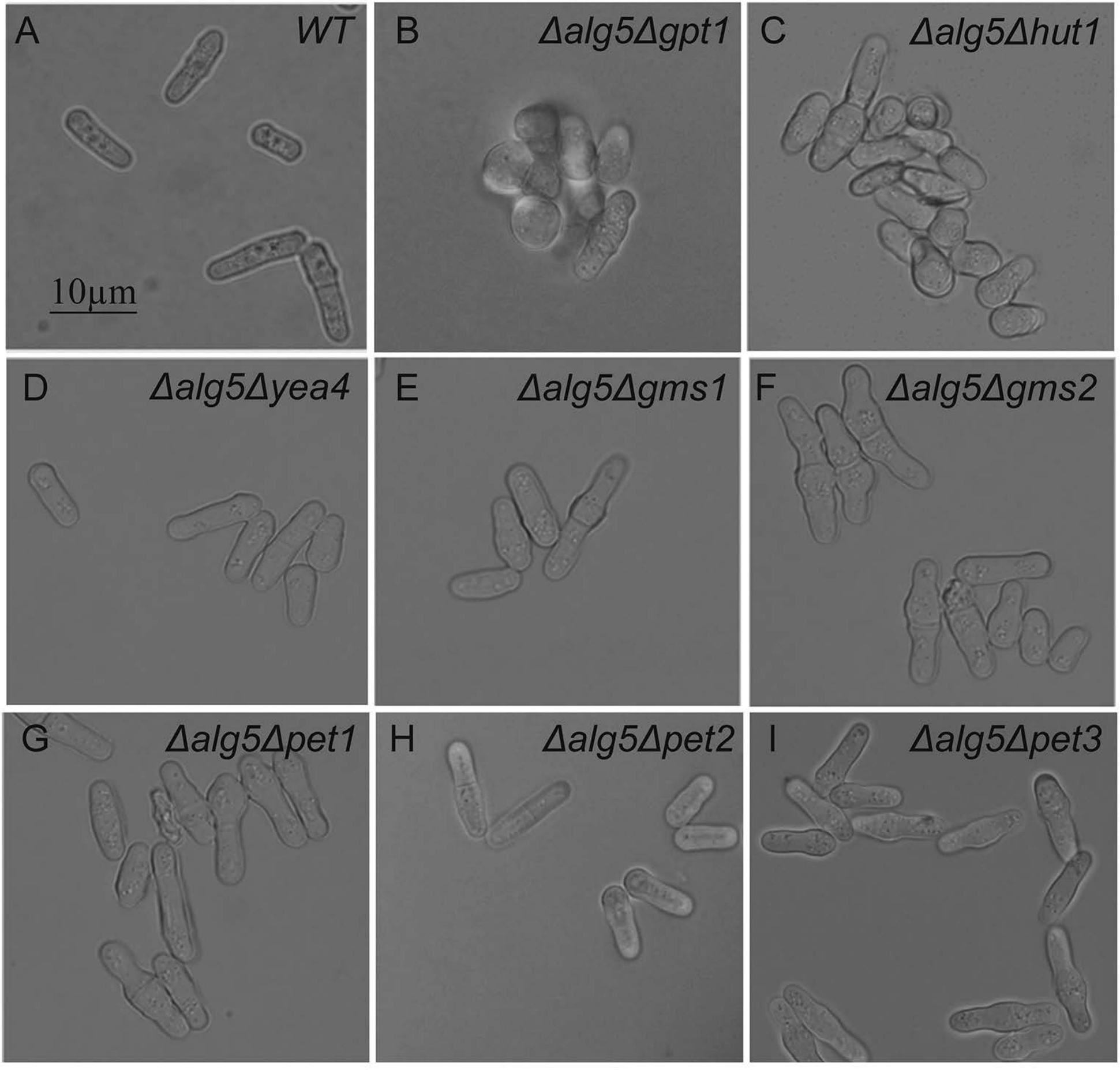
A
WT
10μm
B
Δalg5Δgpt1
C
Δalg5Δhut1
D
Δalg5Δyea4
E
Δalg5Δgms1
F
Δalg5Δgms2
G
Δalg5Δpet1
H
Δalg5Δpet2
I
Δalg5Δpet3

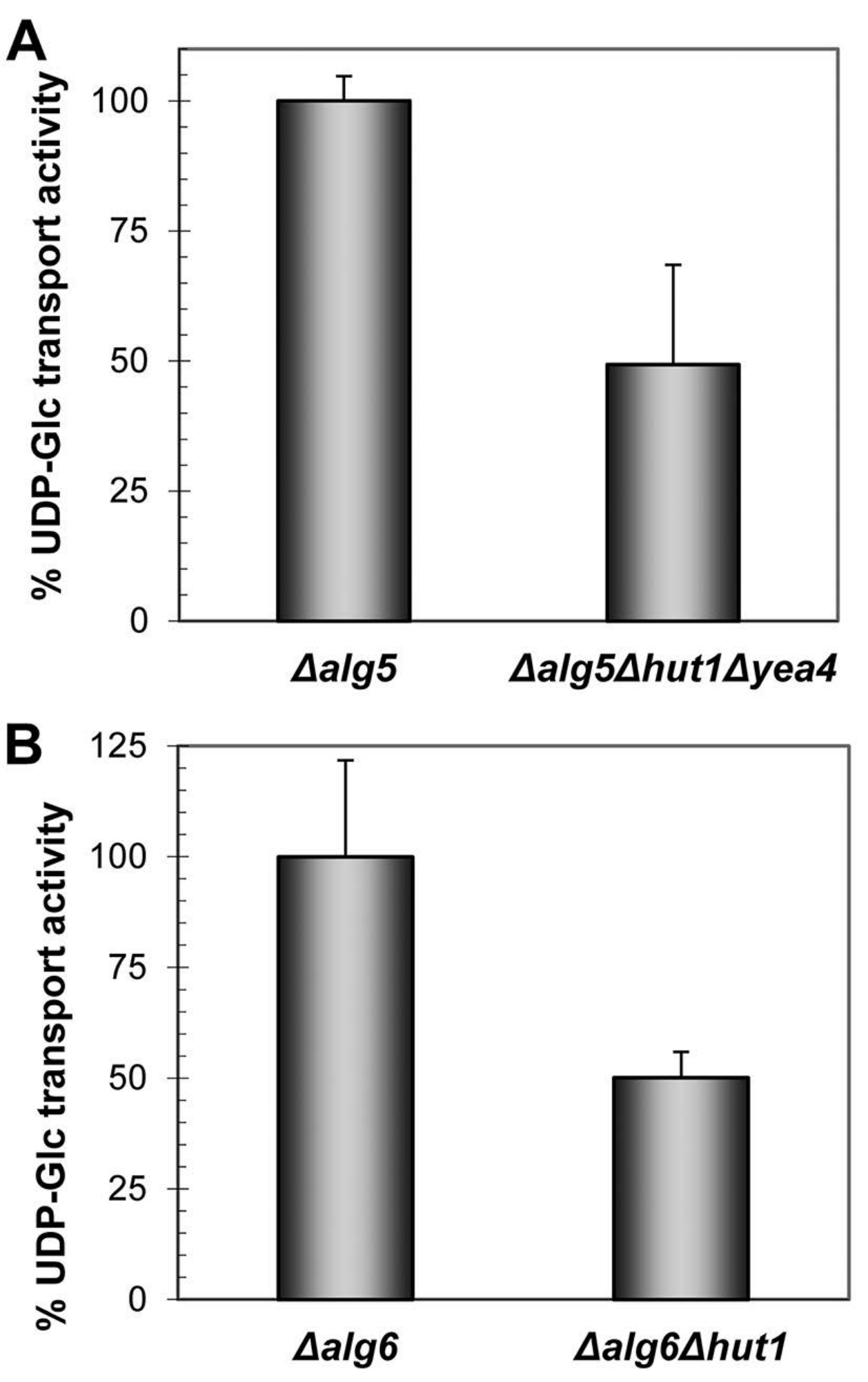
A
% UDP-Glc transport activity
100
75
50
25
0
Δalg5
Δalg5Δhut1Δyea4
B
% UDP-Glc transport activity
125
100
75
50
25
0
Δalg6
Δalg6Δhut1

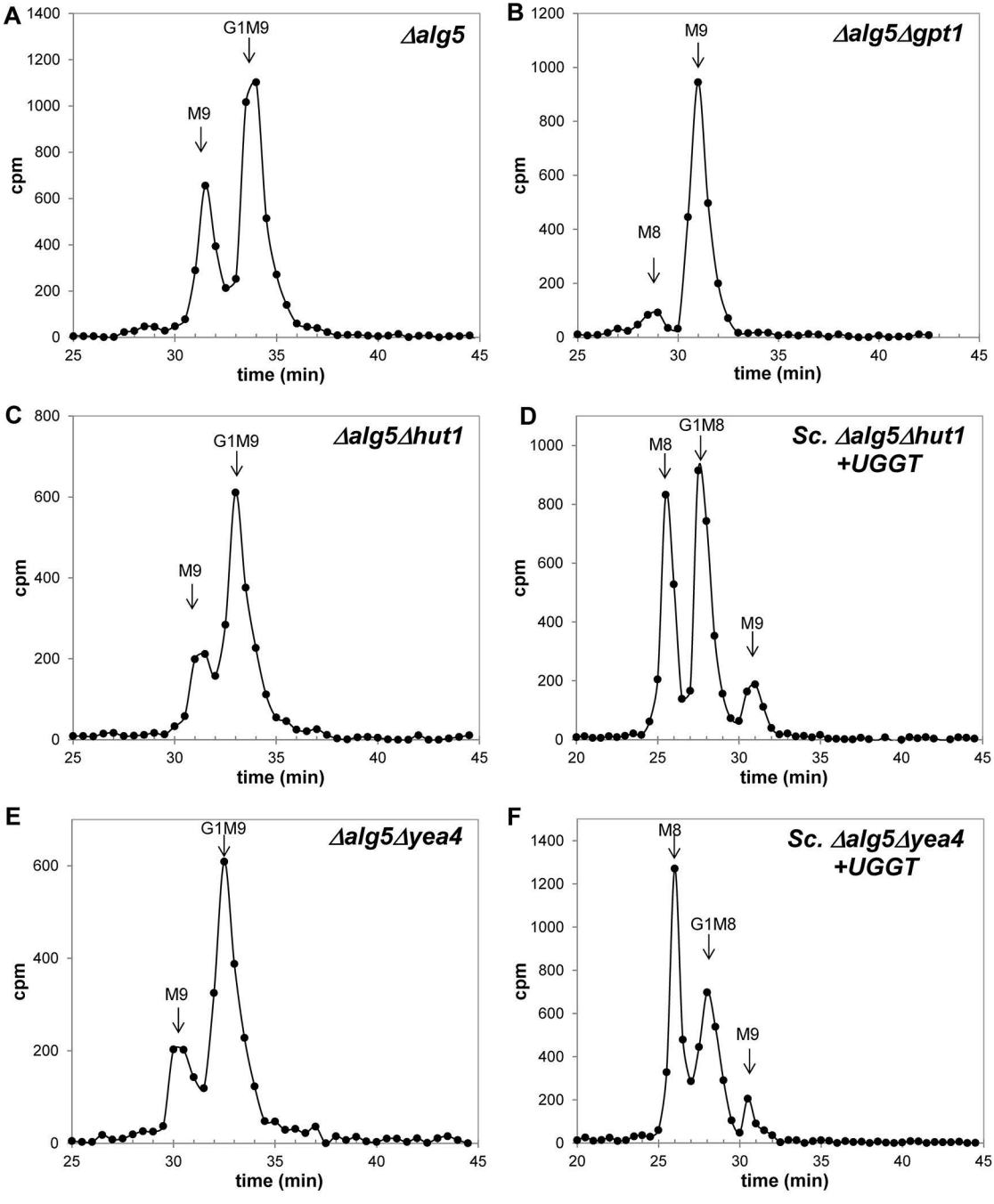
A
Δalg5
G1M9
M9
cpm
time (min)
B
Δalg5Δgpt1
M9
M8
cpm
time (min)
C
Δalg5Δhut1
G1M9
M9
cpm
time (min)
D
Sc. Δalg5Δhut1
+UGGT
M8
G1M8
M9
cpm
time (min)
E
Δalg5Δyea4
G1M9
M9
cpm
time (min)
F
Sc. Δalg5Δyea4
+UGGT
M8
G1M8
M9
cpm
time (min)

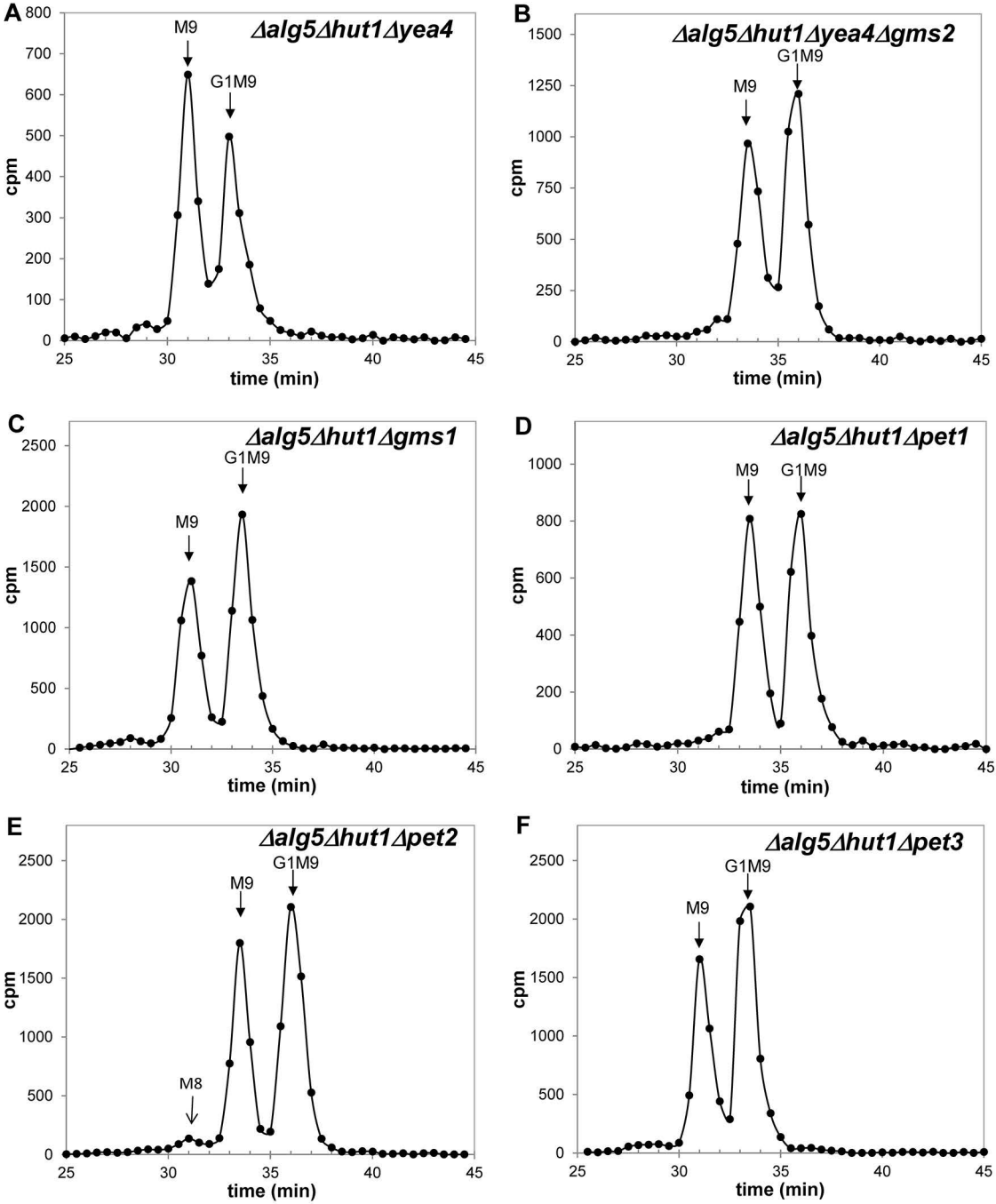
A
Δalg5Δhut1Δyea4
M9
G1M9
cpm
time (min)
B
Δalg5Δhut1Δyea4Δgms2
M9
G1M9
cpm
time (min)
C
Δalg5Δhut1Δgms1
M9
G1M9
cpm
time (min)
D
Δalg5Δhut1Δpet1
M9
G1M9
cpm
time (min)
E
Δalg5Δhut1Δpet2
M8
M9
G1M9
cpm
time (min)
F
Δalg5Δhut1Δpet3
M9
G1M9
cpm
time (min)

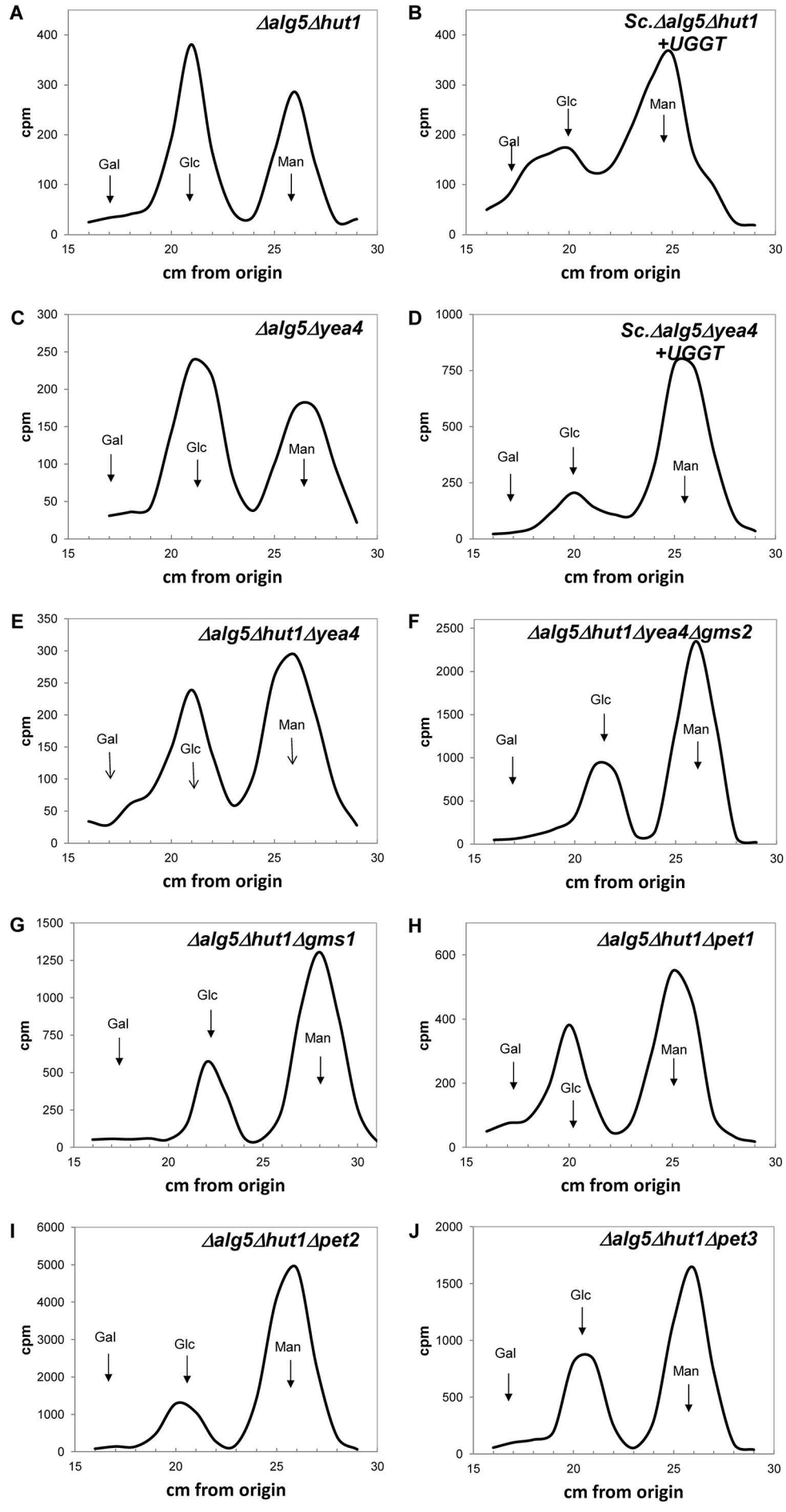
A
Δalg5Δhut1
cpm
cm from origin
Gal
Glc
Man
B
Sc.Δalg5Δhut1
+UGGT
C
Δalg5Δyea4
D
Sc.Δalg5Δyea4
+UGGT
E
Δalg5Δhut1Δyea4
F
Δalg5Δhut1Δyea4Δgms2
G
Δalg5Δhut1Δgms1
H
Δalg5Δhut1Δpet1
I
Δalg5Δhut1Δpet2
J
Δalg5Δhut1Δpet3